INFORMATION TO USERS

This manuscript has been reproduced from the microfilm master. UMI films the text directly from the original or copy submitted. Thus, some thesis and dissertation copies are in typewriter face, while others may be from any type of computer printer.

The quality of this reproduction is dependent upon the quality of the copy submitted. Broken or indistinct print, colored or poor quality illustrations and photographs, print bleedthrough, substandard margins, and improper alignment can adversely affect reproduction.

In the unlikely event that the author did not send UMI a complete manuscript and there are missing pages, these will be noted. Also, if unauthorized copyright material had to be removed, a note will indicate the deletion.

Oversize materials (e.g., maps, drawings, charts) are reproduced by sectioning the original, beginning at the upper left-hand corner and continuing from left to right in equal sections with small overlaps. Each original is also photographed in one exposure and is included in reduced form at the back of the book.

Photographs included in the original manuscript have been reproduced xerographically in this copy. Higher quality 6" x 9" black and white photographic prints are available for any photographs or illustrations appearing in this copy for an additional charge. Contact UMI directly to order.

UMI

A Bell & Howell Information Company
300 North Zeeb Road, Ann Arbor MI 48106-1346 USA
313/761-4700 800/521-0600

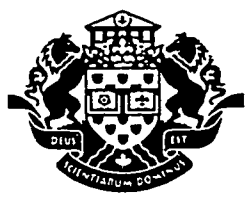

Université d'Ottawa · University of Ottawa

Study of Fluorosilicone Rubber Membrane for Pervaporation

Kin-Yip Charles Tsang

A thesis submitted to the School of Graduate Studies and Research
in partial fulfilment of the requirements for the degree of
Master of Applied Science
in the Department of Chemical Engineering
University of Ottawa

September 1998

National Library of Canada
Acquisitions and Bibliographic Services
395 Wellington Street
Ottawa ON K1A 0N4
Canada

Bibliothèque nationale du Canada
Acquisitions et services bibliographiques
395, rue Wellington
Ottawa ON K1A 0N4
Canada

Your file Votre référence

Our file Notre référence

0-612-36749-5

Canada

Abstract

Homogeneous fluorosilicone rubber membranes were prepared to study the dehydration of isopropyl alcohol by pervaporation. The membranes were either water-selective or isopropyl alcohol-selective, depending on the feed composition. The azeotropic composition of isopropyl alcohol-water system predicted using Margules Equation occurred at 41 mole% of water. However, the feed and permeate compositions were found to be equal in pervaporation experiments when the water content in the feed was approximately 70 mole%. Generally, water-selectivity was enhanced by pervaporation as compared to liquid-vapor equilibrium.

Composite membranes were also prepared with a thin layer of fluorosilicone rubber coated on top of a porous substrate polyethersulfone membrane. It was found that the performance of the composite membrane was affected by the molecular weight of polyethersulfone used to prepare the porous substrate. The performance of composite membrane became more consistent as the molecular weight of polyethersulfone became more uniform. The membrane selectivity increased with a decrease in the mean pore size.

Sommaire

Plusieurs membranes composées d'élastomères de fluorsilicone homogène furent préparées afin d'étudier la deshydration de l'alcool isopropylique. Les membranes étaient soit selective à l'eau ou à l'alcool isopropylique, dépendant de la composition de l'alimentation. La composition azéotropique du système alcool isopropylique-eau fut prédit par l'équation de Margules qu'elle serait à 41 mole % d'eau. Par contre, la composition de l'alimentation et du permeat étaient égales dans des expériences de pervaporation lorsque l'eau contenu dans l'alimentation était de 70 mole %. Généralement, la séléctivité d'eau fut améliorée par la pervaporation si comparé à l'équilibre liquide-vapeur.

Des membranes du type composite furent aussi préparées en apposant une mince couche de fluorosilicone caoutchouté au dessus d'une membrane au substrat poreuse fait en sulfone polyethérique. Il a été trouvé que la performance de la membrane en composite fut affecté par le poid moléculaire du sulfone polyethérique utilisé durant la preparation du substrat poreu. La membrane en composite est devenue plus stable lorsque le poid moléculaire du sulfone polyethérique atteigna une meilleure uniformitée. La séléctivité de la membrane augmenta avec une diminution de la grandeure moyenne des pores.

Acknowledgements

I would like to thank Dr. T. Matsuura for his supervision, and his experience and insight contributed to this study. I also greatly appreciate the encouragement and inspiration that he gave me during my study. I would like to thank Anachemia Solvents (Mississauga, Ontario) for the financial support, and National Research Council (Institute for Chemical Process and Environmental Technology, Ottawa) for the supply of equipment and technical support. Also, I would like to thank Mr. Louis Tremblay, Mr. Frank Ziroldo, and Mr. Gérard Nina for their technical advice and time given for the design and preparation of my equipment. Furthermore, I would like to thank the fellow students and researchers at the Industrial Membrane Research Institute for the sharing of laughter and ideas. Finally, I would like to thank my friends, Josiah, Amanda, and Asoun for their company in the laboratory many late nights.

This thesis is dedicated to
my dear Christina who constantly supported me
by prayer and encouraged me throughout my graduate study.

Table of Contents

List of Figures

List of Tables

Nomenclature

a	Einstein-Stokes radius in Section 3.1 (m), and Mark-Houwink Constant in Section 5.1 (dimensionless)
$\underline{a}$	Geometric mean of Einstein stokes radius of solute molecules (m)
A	A constant defined by Equation (14) in Section 3.2 (mole/s kg)
A_o	Intercept of linear regression on log-normal probability plot (dimensionless)
A_1	Slope of linear regression on log-normal probability plot (m^{-1})
A_{mixt}	A constant defined by Equation (14) in Section 3.2 for a mixture of solution (mole/s kg)
B	A constant defined by Equation (20) in Section 3.2 (mole m s^3/kg^2)
B_i	A constant defined by Equation (20) in Section 3.2 for the ith component in a mixture of solution (mole m s^3/kg^2)
B_j	A constant defined by Equation (20) in Section 3.2 for the jth component in a mixture of solution (mole m s^3/kg^2)
c	concentration of polymer solution for intrinsic viscosity measurement (kg/m^3)
c_{A2}	Molar concentration of solute present at the concentrated boundary solution on the high pressure side of membrane ($mole/m^3$)
c_{A3}	Molar concentration of permeated product solution on the atmospheric side of membrane ($mole/m^3$)
D	Diffusivity (m^2/s)

f'	Solute separation based on the solute concentration in the boundary phase defined by Equation (dimensionless) in Section 3.1 (dimensionless)
k	Boltzmann Constant in Section 3.1 (J/K), and permeability coefficient in Section 3.2 (m^2)
k_H	Henry's constant (mole/kg Pa)
k_H'	(Unit weight of polymer/volume of adsorbed gas molecules) × k_H (mole/m^3 Pa)
K	Mark-Houwink Constant (m^3/kg)
M	Molecular weight (g/mole)
N_t	Total number of pores per effective membrane area (dimensionless)
P	Pressure (Pa)
P_2	Pressure at the pore inlet (Pa)
P_3	Pressure at the pore outlet (Pa)
P^*	Saturation vapor pressure (Pa)
P_i^*	Vapor pressure of the ith component in the saturated vapor (Pa)
$P_{i,3}$	Vapor pressure of the ith component at the pore outlet (Pa)
P_j^*	Vapor pressure of the jth component in the saturated vapor (Pa)
$P_{j,3}$	Vapor pressure of the jth component at the pore outlet (Pa)
Q_{liq}	Molar flux per effective membrane area for liquid phase (mole/s m^2)
$Q_{liq,i}$	Molar flux per effective membrane area in liquid phase for the ith component (mole/s m^2)
Q_{vap}	Molar flux per effective membrane area for vapor phase (mole/s m^2)

$Q_{vap,j}$	Molar flux per effective membrane area in vapor phase for the jth component (mole/s m^2)
r	Pore radius (m)
R	Gas law constant (Pa/mole K)
$\underline{R}$	Mean pore radius (m)
R^*	Rejection coefficient (dimensionless)
t	Thickness of the adsorption monolayer in Section 3.2 (m), and time required for a polymer solution traveling between two points in capillary tube of a viscometer in Section 4.9 (s)
t_o	Time required for a pure solvent traveling between two points in the capillary tube of a viscometer (s)
T	Temperature (K)
u_b	Velocity of solvent in the pore (m/s)
x	Amount of gas adsorbed in a given amount of the membrane material (mole/kg)
$y_{i,3}$	Mole fraction of the ith component at the pore outlet (dimensionless)
$Y(r)$	Normal pore size distribution function (m^{-1})

Greek letters

α	separation factor (dimensionless)
δ	The total length of the pore (m)
δ_a	The length of the liquid-filled portion of the pore (m)
δ_b	The length of the vapor-filled portion of the pore (m)

η	Solvent viscosity in Section 3.1 (Pa s), and liquid viscosity in Section 3.2 (Pa s)
$[\eta]$	Intrinsic viscosity (m^3/kg)
η_{sp}	Specify viscosity (dimensionless)
θ	Sieving coefficient (dimensionless)
μ	Surface viscosity of the adsorption layer of vapor (Pa s)
ρ	Density of liquid (kg/m^3)
σ	Standard deviation of normal pore radius distribution (m)
σ_a	Geometric standard deviation of Einstein-Stokes radius (dimensionless)
τ	Argument of the error function in terms of a, $\underline{a}$, and σ_a (dimensionless)

Abbreviations

Dissolved PES	The fraction of PES (Victrex 200p), the low molecular weight polyethersulfone dissolved in chloroform
ESR	Einstein-Stokes radius (m)
FPES membrane	Polyethersulfone membrane made of undissolved PES
NMP	N-methylpyrrolidone
PEG	Polyethylene glycol
PES	Polyethersulfone
PES membrane	Polyethersulfone membrane made of untreated PES
PES (Victrex 200p)	Commercial polyethersulfone polymer named as Victrex 200p
PVP	Polyvinylpyrrolidone

Undissolved PES	The fraction of PES (Victrex 200p), the high molecular weight polyethersulfone not dissolved in chloroform
Untreated PES	PES (Victrex 200p) not treated by chloroform
PWP	Pure water permeation (mole/s)

1.0 Introduction

Membrane separation processes are regarded as new processes in chemical engineering and are under active development. They include reverse osmosis, nanofiltration, ultrafiltration, gas separation, electrodialysis, and pervaporation. Pervaporation is relatively new among them. These processes are broadly applied in various areas including purification, concentration, and fractionation of fluid mixtures. Dehydration of organic solvent by pervaporation is one of the actively researched areas in membrane separation technologies. In pervaporation, the upstream side of membrane is maintained in contact with a body of liquid containing single or multiple components while vacuum or a sweeping gas stream is applied on the downstream side of the membrane. The body of liquid permeates into the membrane and vaporizes somewhere between the upstream and downstream side of the membrane. This vapor-permeant then moves towards the downstream side of the membrane where it can be collected by condensation or discharged to the ambience. A schematic diagram of this process is shown in Figure 1.1. Besides vacuum and sweeping gas pervaporation, other types of pervaporation include thermal pervaporation (Franken et al., 1990, and Neel, 1991), perstraction or osmotic distillation, saturated vapor permeation, pressure-driven pervaporation (Goncalves et al., 1990), and electrically induced pervaporation (Timashev et al., 1994).

Zhu (1997) found recently that composite membranes prepared by coating a thin layer of cross-linked fluorosilicone rubber on the surface of a porous polyethersulfone membrane dehydrate organic solvents effectively by pervaporation. For example, a

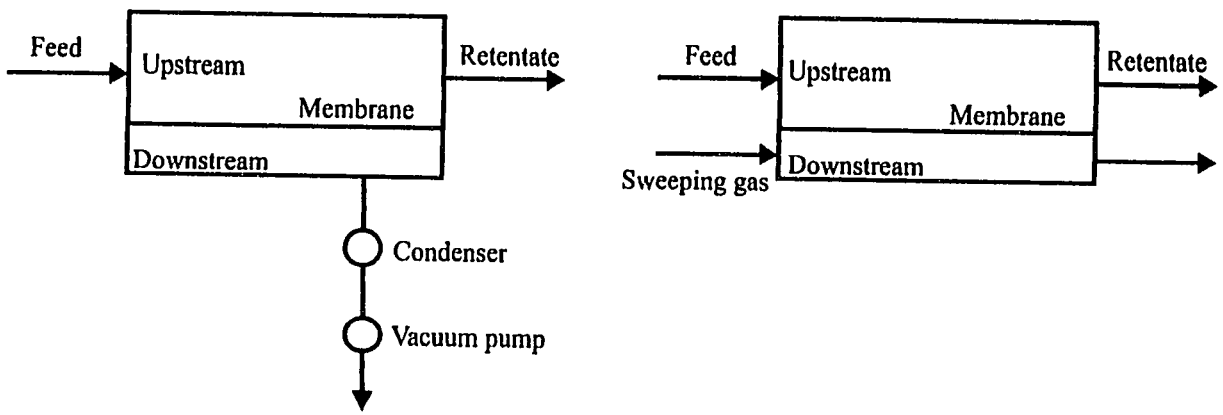

Figure 1.1 Schematic diagram of pervaporation process operated with vacuum or sweeping gas.

separation factor of about 50 was achieved when a water/isopropyl alcohol mixture of 5.7/94.3 by weight was treated by the above composite membrane. The permeate flux was however as low as below 0.1 kg/m^2 h. Realizing the novelty of fluorosilicone rubber as a membrane material, this study was initiated to explore the potential of this new type of membrane for its application in the dehydration of organic solvents.

In his attempts, Zhu used only commercial polyethersulfone membrane as the porous substrate. It is generally accepted, however, that the substrate membrane exerts a strong influence on the overall performance of the composite membrane. Therefore, an attempt was made in this work to prepare porous polyethersulfone membranes under different conditions, and these membranes were used to make the composite membranes. Two variables were considered in the preparation of porous polyethersulfone membranes. One is the uniformity in the molecular weight distribution of polyethersulfone polymer and the other was the pore size and the pore size distribution of the polyethersulfone membrane. The objectives of this work are shown below:

1. To study the dehydration properties of the homogeneous fluorosilicone rubber membrane.
2. To study the effect of the uniformity of the molecular weight of polyethersulfone polymer on the performance of the composite fluorosilicone rubber membranes and polyethersulfone membranes, whereby the uniformity of the molecular weight distribution is increased by removing the low molecular weight fraction of the polymer using an appropriate solvent.

3. To study the effect of the pore size of the substrate polyethersulfone membrane on the performance of the composite fluorosilicone rubber membranes, whereby the pore size is changed by changing the composition of the casting solution.

2.0 Literature Survey

The concept of pervaporation can be traced back to 1917. This phenomenon was observed by Kober (1917). He reported the selective permeation of water from aqueous solutions of albumin and toluene through collodion (cellulose nitrate) film. Then, Heisler et al. (1956) published their results for separation of water/ethanol mixtures using a cellulose membrane. This was the first publication for the dehydration of organics. Although research was continued (Binning and James, 1958, Binning et al., 1961 and 1962), no membrane could be commercialized because of the low permeation flux. In early 1980s, Gesellschaft für Trenntechnik (GFT) Co. made a breakthrough by developing a composite membrane comprising a thin layer of cross linked polyvinyl alcohol supported on a porous polyacrylonitrile substrate. A pervaporation process for ethanol dehydration was then commercialized. Currently, two applications using pervaporation have been commercialized: dehydration of alcohols and other solvents, and removal of small amounts of organic compounds from contaminated waters.

2.1 Membrane Materials Developed for Pervaporation Dehydration

There are three types of polymers utilized to make polymeric membrane: glassy polymers, rubbery polymers (elastomeric polymers), and ionic polymers. The glassy polymer is differentiated from rubbery polymer by their state at room temperature. A polymer is considered as glassy polymer if it is in glassy state at room temperature. On the other hand, a polymer is considered as rubbery (elastomeric) polymer if it is in amorphous state at room temperature. Ionic polymer can be glassy or rubbery because a

polymer is considered as ionic if the polymer carries ionic groups. Overall, glassy and ionic polymers are used to make water-selective membranes applied in solvent dehydration, and rubbery polymers are used to make organics-selective membranes applied in removal of organic compounds from water. Materials with low hydrophilicity generally yield low water-flux membrane, and the ones with high hydrophilicity yield high water flux. However, high hydrophilicity materials such as polyvinyl alcohol and polyacrylic acid require cross-linking to improve stability and selectivity. The key factor is to maintain a balanced hydrophilicity and hydrophobicity. Huang (1991) discussed the techniques of controlling this balance.

The most popular materials for making dehydration membranes are polyvinyl alcohol and polyacrylic acid. Chitosan and aromatic polyimide also attract great attention. Polyvinyl alcohol-based membrane has been studied most intensively. The focus was on its modification to improve the permselectivity and stability, and the membrane was used for various applications (Huang, 1991). Polyacrylic acid has a high charge density due to the carboxyl groups. The polyacrylic acid-based membranes are being developed by BP International of U.K. and Daicel Chemical of Japan for solvent dehydration. Chitosan is a N-deacetylated product of Chitin. It is a linear polymer comprised primarily of glucosamine, and it is the second most abundant natural polymer (next to cellulose). Chitosan membranes have high solvent stability and high selectivity for water. Chemically modified chitosan has been studied by Lee for separation of ethanol/water and acetic acid/water mixtures (Lee, 1993, Lee and Shin, 1991d, Lee et al., 1991a-c, 1992). Aromatic polyimides are known for their thermal stability, mechanical

strength, and chemical resistance. Various aromatic polyimide-based membranes for dehydration of organic solvent and separation of organic mixtures are being developed by Ube Industries of Japan.

2.2 Fluorosilicone Rubber and Polyethersulfone as Composite Membrane Materials

Fluorosilicone rubber, also known as polytrifluoropropylmethylsiloxane, is a new material used as membrane material. There is no publication reported for any membranes made of it. It has a basic structure that is similar to polydimethylsiloxane and carries a trifluoropropyl group. Polydimethylsiloxane membranes are mainly used for the selective permeation of organic compounds from aqueous solutions, whereas the fluorosilicone-rubber-based membranes are expected to exhibit a water-selective characteristic because of the existence of trifluoropropyl groups (a polar group) on the polymer backbone. Fluorosilicone rubber offers great physical and chemical advantages to be used as the membrane material. Laboratoire de Recherches et de Contrôle du Caoutchouc in France conducted a study on the physical and chemical properties of this material and reported the results in one of their publications (LRCC, 1983). The report described the chemical structure of the fluorosilicone rubber as shown in Figure 2.1. This material, as reported, has high resistance to oils, fuels, chemicals, and high temperature. The vulcanized fluorosilicone rubber has good resistance to esters, chlorinated hydrocarbons, ozone and oxygen. It shows only a small degree of swelling in alcohols. However, it is susceptible to hydrolysis by acids and bases because of its polarity contributed by the trifluoropropyl

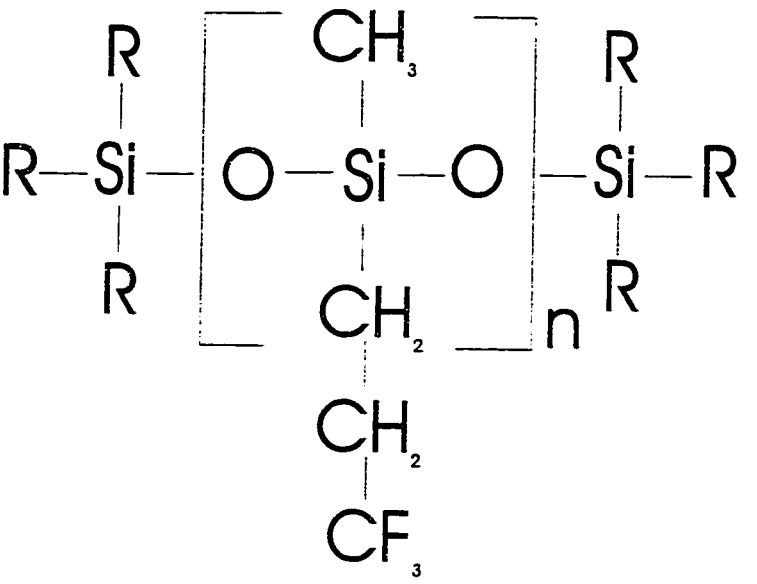

Figure 2.1 Chemical formula for fluorosilicone rubber (LRCC, 1983). 'n' is approximately 5000 and 'R' is a methyl or functional group.

branch existing in the molecule. In terms of temperature, fluorosilicone rubber has a wide range of service temperature. Its glass transient state temperature is -65°C and its maximum service temperature is 230°C at which the material starts to decompose. Therefore, fluorosilicone rubber is a versatile polymeric material that can offer its many advantages to be used as membrane material. Polyethersulfone has good thermal stability, excellent mechanical and electrical properties, and good stability to water, acid and many chemicals (Osawa, 1986). Lu and Gao (1994) also concluded in their study that membranes made of polyethersulfone have good thermal and chemical stability since its glass transition temperature is as high as 230°C. They immersed the polyethersulfone membranes in water (100°C from 5 to 60 minutes), in solutions of hydrochloric acid

(pH 2.0), sodium hydroxide (pH 12), hydrogen peroxide (1%), and hypochlorite (500 ppm) before the membranes were tested for pure water permeation. The results showed that the membranes maintained stable water permeation although they were treated in these harsh environments. The chemical formula of polyethersulfone is shown in Figure 2.2.

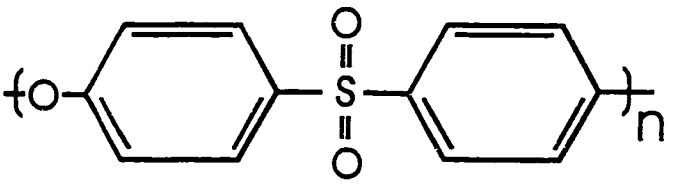

Figure 2.2 Chemical formula for polyethersulfone.

Tam et al. (1993) carried out a brief test to test solubility of polyethersulfone in various solvents. He observed that the polyethersulfone (Victrex 200p) mixed with chloroform formed a cloudy mixture. This indicates that chloroform may be a potential solvent that can be used for dissolving the low molecular weight fraction from the bulk of the polymer. Lafrenière et al. (1987) reported that polyethersulfone membranes have various mean pore sizes when the membranes were prepared from casting solutions with different concentrations. In their study, they fabricated various ultrafiltration membranes using twenty-one different polymer solution concentrations. These membranes were then subjected to ultrafiltration tests using polyethylene glycols of molecular weights from 300 to 15000. They determined the pore size distribution of the membrane by applying transport equations developed from the surface force-pore flow model (Sourirajan and

Matsuura, 1985) to the ultrafiltration separation data of polyethylene glycols. The best pore size distribution was evaluated by optimizing the agreement of calculated and experimental separation data.

2.3 Asymmetric and Composite Flat-Sheet Membranes

Asymmetricity is introduced into the membrane structure in order to reduce the effective thickness and the hydrodynamic resistance of the membrane. The asymmetricity is generally arranged in a way that a thin dense skin layer is supported on the top of a microporous substrate. Asymmetric membranes have two categories: one is integrally skinned asymmetric membrane (often simply called asymmetric membrane) made of a single material, and the other is composite membrane consisting of a skin layer and a substrate layer which are made from two different materials.

2.3.1 Asymmetric Membranes

For asymmetric membranes, several techniques have been developed to achieve the asymmetricity (Wijman and Smolders, 1986). They include precipitation from the vapor phase, controlled evaporation, immersion in a non-solvent, thermal precipitation, and a combination of the techniques mentioned above. However, the immersion precipitation technique developed by Loeb and Sourirajan (1960) is the most commonly used technique. The variables involved in this fabrication process and their effects on the structure of the resulting membranes were described by Kesting (1985). Many works involving different polymers have been devoted to study and analyze the effects of

membrane preparation conditions on the performance of the integrally skinned asymmetric membranes produced by the immersion precipitation technique, also called gelation or nonsolvent-solvent exchange. They were carried out by Maeda et al. (1991), Lai et al. (1994), Tanihara et al. (1992), Yanagishita et al. (1994, 1995), Huang and Feng (1993a, b), Li et al. (1994), and Jian and Pintauro (1993).

A resistance model for pervaporation has been developed by Huang and Feng (1993b). In the above model, resistance to the mass flow in a membrane is considered analogous to the resistance to the electric-current flow in a circuit. This model is not a mechanistic approach to membrane separation, but it offers a correlation between membrane selectivity and resistance components lying in the path of mass transport through the membrane.

2.3.2 Composite Membranes

Preparation of composite membranes involves casting of the microporous support and deposition of the selective dense layer (barrier) on the surface of the support. Three methods have been developed to fabricate composite membranes (Heinzelmann, 1991). They include casting of the barrier layer and the microporous support separately, followed by lamination; direct coating of a polymer solution onto the microporous support, followed by a post treatment; and in situ formation of the barrier layer on a microporous support film. Among these three methods, direct coating is the most commonly used preparation method for the composite membrane. The microporous support layer is required to be highly porous but the pores should be sufficiently small to prevent the

coating solution from filling the pores since filling the pores will result in flux reduction. Several parameters will affect the coating process. They are composition, viscosity, and surface tension of the coating solution; the pre-treatment of the support; choice of coating methods such as dip coating, spray coating, and spin coating; and the drying conditions. Many studies were conducted to study the performance and characteristics of, and the separation mechanism in composite membranes. For examples, Bai et al. (1993) studied the acetic acid/water separation by polydimethylsiloxane-coated (PDMS-coated) asymmetric polyetherimide membranes; Deng et al. (1994) studied the acetic acid/water separation by an asymmetric polyamide membrane laminated with a PDMS layer; Fudematsch et al. (1991) studied the influence of composite membrane structure on pervaporation; Heintz and Stephan (1994a and b) proposed a general solution-diffusion model for composite membrane that takes concentration polarization, coupled diffusion through the dense skin layer, and the influence of the porous support into consideration. However, the separation mechanism occurring in pervaporation membrane is still not fully understood.

2.4 The Transport Model

There are two models describing the mass transport of the pervaporation process: the solution-diffusion model and the pore flow model. According to the solution-diffusion model, there are three consecutive steps in mass transport (Kataoka et al., 1991, and Wijmans and Baker, 1995): sorption of the permeant from the feed (liquid) to the membrane, diffusion of permeant in the membrane, and the desorption of permeant to the

vapor phase on the downstream side of the membrane. According to the pore flow model, there are also three consecutive steps in mass transport (Okada and Matsuura, 1991 and 1992, and Okada et al., 1991). They are liquid transport from the pore inlet to a liquid-vapor phase boundary, evaporation at the phase boundary, and vapor transport from the phase boundary to the pore outlet.

For the solution-diffusion model, pores are not considered to exist in the membrane. The transport takes place in penetrant-scale transient gaps generated by the thermally agitated motion of chain segments comprising the polymer matrix. Therefore, diffusion of penetrant takes place from the upstream to the downstream through the membrane. However, the permeation is the result of the random jumps of the penetrant in the membrane. For the pore flow model, pores are defined as the space between non bound material entities in the polymer matrix. The radius of the pore is expressed by a distance greater than zero. The transport takes place in these pores in the membranes. The flow mechanism in these pores is expressed by Darcy's equation for the liquid transport, and by surface flow for the vapor transport. The pore model is a relatively new theory and in a preliminary stage. On the other hand, the solution-diffusion model received much attention and many publications had been written for it. Some important contributions are Fels and Huang (1971), Lee (1975), Greenlaw et al. (1977), Brun et al. (1985a and b), Mulder and Smolders (1984), Mulder et al. (1985a, b and 1986), Blume et al. (1990), Rhim and Huang (1989, 1992), Huang and Rhim (1992), Yeom and Huang (1992), and Doong et al. (1995). In this work, the experimental data will be analyzed using the pore flow model.

3.0 Theory

3.1 Mean Pore Size and Pore Size Distribution of Ultrafiltration Polyethersulfone Membrane

The morphological structure of polymeric membrane can be described as clusters of 'nodules' put together. The spaces between these nodules are considered as 'pores' or 'free volumes' which allow molecules pass through. According to the Surface Force-Pore Flow Model (Sourirajan and Matsuura, 1985), the uniformity (in terms of shape and size) of these pores is very important for the skin layer of asymmetric membrane where solute separation is believed to take place. From the model, the solute separation, f', is defined as

$$f' = 1 - \frac{\textit{product solute concentration}}{\textit{feed solute concentration in the boundary phase}} \tag{1}$$

f' can be evaluated by the following two equations (Sourirajan, 1985)

$$f' = 1 - \frac{1}{c_{A2}} \frac{\int_0^\infty Y(r) \left[\int_0^R c_{A3}(r)\, u_B(r)\, r\, dr \right] dr}{\int_0^\infty Y(r) \left[\int_0^R u_B(r)\, r\, dr \right] dr} \tag{2}$$

$$Y(r) = \frac{1}{\sigma \sqrt{2\pi}} \exp\left[- \frac{(r - \underline{R})^2}{(2\sigma^2)} \right] \tag{3}$$

It is obvious that the mean pore radius, $\underline{R}$, and the standard deviation of normal pore radius distribution, σ, are responsible for determining the value of f', if all other parameters are unchanged. Although the method of obtaining $\underline{R}$ and σ are described in detail (Sourirajan and Matsuura, 1985), the method looks too complicated. Therefore, the average pore size and standard deviation are determined by the method proposed by Michaels (1980). His method uses two parameters, the geometric mean, $\underline{a}$, and the geometric standard deviation, σ_a, of Einstein-Stokes Radius (ESR), to describe a sieving curve or a rejection curve for an ultrafiltration separation system. Sieving curve is a plot of sieving coefficient versus the ESR, a, of the permeant (polyethylene glycol is the permeant in this study), whereas rejection curve is a plot of rejection coefficient versus the ESR of the permeant. Rejection coefficient (R^*) and sieving coefficient (θ) is a complement of each other and is defined as follows:

$$R^* = 1 - \frac{\textit{solute concentration in the product solution}}{\textit{solute concentration in the feed solution}} \tag{4}$$

$$\theta = 1 - R^* \tag{5}$$

Since the two parameters, $\underline{a}$ and σ_a, involved in the sieving curve or rejection curve are a similitude to the membrane pore size distribution $\underline{R}$ and σ, his method was adopted in this study.

The Einstein-Stokes Radius (ESR) of solute polyethylene glycol molecules of various molecular weights were evaluated by Equation (6).

$$a = \frac{kT}{6\pi\eta D} \tag{6}$$

where a is the ESR of polyethylene glycol, k is Boltzmann constant, T is absolute temperature, η is pure solvent viscosity, and D is diffusivity of polyethylene glycol. The diffusivity can be evaluated by Equation (7), when polyethylene glycol is used as the solute and water as the solvent. (Hsieh et al., 1979; Hsieh et al. 1979; Mandelkern and Flory, 1952).

$$D = \frac{1.2 \times 10^8 \, k \, T}{\eta \left(M[\eta]\right)^{1/3}} \tag{7}$$

where $[\eta]$ is intrinsic viscosity of polyethylene glycol in its aqueous solution, and M is the molecular weight of polyethylene glycol. The intrinsic viscosity can be evaluated by

$$[\eta] = 4.9 \times 10^{-5} \, M^{0.672} \tag{8}$$

as described by Hsieh et al. (1979). Combining Equations (6), (7), and (8), yields

$$a = 1.618 \times 10^{-11} \, M^{0.557} \tag{9}$$

by which ESR of a polyethylene glycol molecule can be evaluated from its molecular weight.

The rejection curve and sieving curve has a characteristic of S-shape. Since the appearance is similar to cumulative-particle-size-distribution curve for particulate solids, Michaels (1980) suggested a log-normal distribution function to correlate the sieving coefficient or rejection coefficient with the ESR of the permeant. According to the log-

normal distribution R^* is given as a function of a by

$$R^* = erf(\tau) = \frac{1}{\sqrt{2\pi}} \int_{-\infty}^{\tau} e^{-\frac{u^2}{2}} du \tag{10}$$

where

$$\tau = \frac{\log\left(\frac{a}{\underline{a}}\right)}{\log \sigma_a} \tag{11}$$

When the R^* obtained from an ultrafiltration experiments is plotted versus the ESR of polyethylene glycol on a log-normal probability scale, a straight line in the form of

$$F(R^*) = A_o + A_1(\ln a) \tag{12}$$

is obtained. A_o and A_i are the intercept and the slope, respectively. From the plot, $\underline{a}$ can be determined at $R^* = 0.5$ (= 50% if it is given as a percentage of separation). Likewise, σ_a can be determined from the ratio of a at 0.159 (15.9%) or 0.8413 (84.13%) and $\underline{a}$, respectively. By considering the assumptions stated below, the mean pore radius ($\underline{R}$) and the standard deviation (σ) of the membrane can be considered to be the same as the mean ESR of the permeant and the mean geometric standard deviation determined from the log-normal scale plot of the rejection curve.

1. The size and the shape of a solute molecule do not depend on whether the solute is in the bulk solution (feed) or in the membrane pore.

2. The transport of a solute molecule is not affected by the interaction force between the solute and membrane.

3. Sieving is the only mechanism for the solute separation.

As mentioned at the beginning of this section, the uniformity of the pores is very important for a membrane to exhibit excellent performance. It may also be important when a membrane is used as a porous substrate to prepare a composite membrane since the uniform pore size on the surface of the support membrane will allow smooth coating of a thin layer, as shown in Figure 3.1.

3.2 Pore-Flow Mechanism for Pervaporation

A transport model for pervaporation based on pore-flow mechanism was proposed by Okada et al. (1991). The prediction of this model agreed well with their experimental data. Also, this model led to a correlation between permeation rate and downstream pressure which is similar to that predicted by the sorption-diffusion model (Greenlaw et al., 1977). Furthermore, the pore flow model described by Okada was applicable to membranes of different pore sizes. Their theory is described in the following.

A bundle of straight cylindrical pores with length δ penetrates through a surface layer of a membrane. In the pore, it is assumed that an isothermal condition is maintained. These pores are partially filled with feed liquid and partially filled with vapor as show in Figure 3.2. In the figure, δ_a is the length of the portion of the pore filled with liquid feed, δ_b is the length of the portion of the pore filled with vapor; P_2 is the

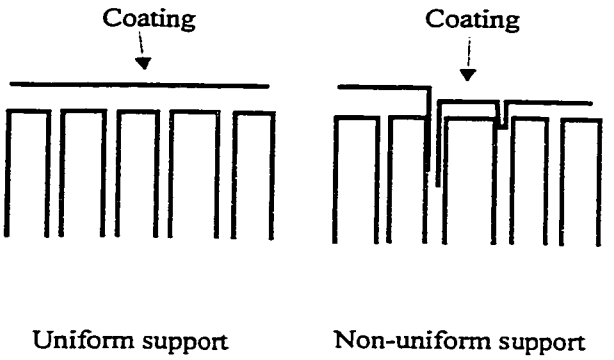

Figure 3.1 **Possible configurations of the composite membrane when the coating layer is supported by a uniform or non-uniform substrate surface.**

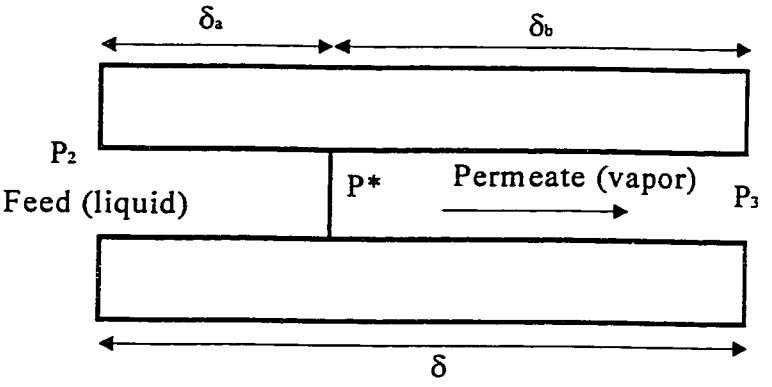

Figure 3.2 **Schematic diagram of pore-flow mechanism for pervaporation occurring in membrane pores.**

pressure of the feed, P_3 is the pressure of the permeate vapor, and P^* is the saturation vapor pressure at the phase boundary. This situation is applicable only if $P_3 < P^*$. The pores would be filled with only liquid if $P_3 \geq P^*$. For a system with a single component of the feed, and $P_3 < P^*$, Darcy's equation is applied to the liquid-filled portion of the cylindrical pore. The liquid flux (Q_{liq}) is expressed as

$$Q_{liq} = \frac{k \rho N_t}{\eta M \delta_a}\left(P_2 - P^*\right) \tag{13}$$

Defining

$$A = \frac{k \rho N_t}{\eta M} \tag{14}$$

Equation (13) can be written as

$$Q_{liq} = \frac{A}{\delta_a}\left(P_2 - P^*\right) \tag{15}$$

For the portion of the pore filled with vapor, three flow-mechanisms can be used to describe the vapor transport in the pores: Viscous flow, Knudsen flow, and Surface flow. Viscous flow happens when the mean free path of the gas molecules is very small relative to the pore diameter. By decreasing the pore diameter of the pores in the membrane, the mean free path of the molecules becomes larger than the pore diameter. This type of flow is called Knudsen flow. When the pore diameter further decreases, no other gas molecules can pass through the membrane pores but only the ones absorbed to wall of

pores. This is called Surface flow. From Surface Flow Model, pore size is assumed small enough that the pore does not allow Knudsen flow. This assumption excludes the superimposition of other gas flow mechanisms. In analogy to Gilliland's surface flow model (Gilliland et al., 1958), the vapor flux (Q_{vap}) is expressed as

$$Q_{vap} \propto \int_{P_3}^{P^*} \frac{x^2}{P} dP \tag{16}$$

where x is the adsorbed amount of vapor and approximated by Henry's equation,

$$x = k_H \, P \tag{17}$$

and k_H is the Henry's Law constant. After substituting Equation (17) into (16) and integrating, (16) becomes

$$Q_{vap} \propto k_H^2 \left(\frac{P^* + P_3}{2} \right) \left(P^* - P_3 \right) \tag{18}$$

A proportionality constant is required for Equation (18). If monolayer adsorption (Chen et al., 1989) is assumed, Equation (18) can be written as

$$Q_{vap} = \frac{\pi \left(2 r t - t^2 \right) t \, N_t}{4 r \, \delta_b} \frac{R T}{\mu} k_H^{'2} \left(\frac{P^* + P_3}{2} \right) \left(P^* - P_3 \right) \tag{19}$$

Defining

$$B = \frac{\pi \left(2 r t - t^2 \right) t \, N_t}{8 r} \frac{R T}{\mu} k_H^{'2} \tag{20}$$

Equation (19) can be simplified to

$$Q_{vap} = \frac{B}{\delta_b}\left(P^{*2} - P_3^2\right) \tag{21}$$

At a steady state, the liquid flux is equal to the vapor flux. Equation (15) is therefore equated to Equation (21). Also,

$$\delta = \delta_a + \delta_b \tag{22}$$

Combining Equation (15), (21), and (22), the molar permeate flux becomes

$$Q = \frac{A}{\delta}\left(P_2 - P^*\right) + \frac{B}{\delta}\left(P^{*2} - P_3^2\right) \tag{23}$$

The first term of Equation (23) expresses the flux of flowing liquid in the membrane pore, whereas the second term expresses the flux of flowing vapor in the membrane pore. Within these two terms, A/δ and B/δ are direct measures of how the flux of permeate responses to the change of the driving force (the pressure-difference). When $P_3 \geq P^*$, the entire pore is filled with liquid. The vapor term is eliminated and Darcy's equation should be applicable from the pressure at the pore inlet, P_2, to the pressure at the pore outlet, P_3. Therefore, the second term of Equation (25) is neglected, and Equation (24) is obtained.

$$Q = \frac{A}{\delta}\left(P_2 - P_3\right) \tag{24}$$

Equation (24) shows that A/δ can be determined by performing a regression analysis for

a linear Q and P_3 correlation obtained experimentally under the condition $P_3 > P^*$. P_2 is atmospheric pressure and constant. Similarly, Equation (23) shows that B/δ can be determined by performing a regression analysis if corresponding Q and P_3 are known from the experiment under the condition $P_3 < P^*$. P^* can be obtained from relevant handbooks, and A/δ is predetermined.

For a system consisting of a binary mixture (i and j) as the feed and $P_3 < P^*$, an equation similar to Equation (15) is valid if there is no separation occurring in the liquid phase in the pore. Using $P_2 - P^*$ as a driving force (Matsuura and Sourirajan, 1989),

$$Q_{liq} = \frac{A_{mixt}}{\delta_a}\left(P_2 - P^*\right) \tag{25}$$

Furthermore, equations analogous to Equation (21) are valid if partial pressures of ith and jth component are considered.

$$Q_{vap,i} = \frac{B_i}{\delta_b}\left(P_i^{*2} - P_{i,3}^{\ 2}\right) \tag{26}$$

$$Q_{vap,j} = \frac{B_j}{\delta_b}\left(P_j^{*2} - P_{j,3}^{\ 2}\right) \tag{27}$$

In Equations (26) and (27), it is assumed that there exists no interaction between the ith and jth components in the surface flow. Then B_i and B_j evaluated from the pure feed data would be applicable in Equations (26) and (27). If any change occurs in the values of B_i and B_j from a single component to a binary mixture system, it can be considered as an

effect of the interaction between the ith and jth component. Since

$$y_{i,3} = \frac{Q_{vap,i}}{Q_{vap,i} + Q_{vap,j}} \tag{28}$$

by substituting Equations (26) and (27) into (28), it becomes

$$y_{i,3} = \frac{B_i \left(P_i^{*2} - P_{i,3}{}^2 \right)}{B_i \left(P_i^{*2} - P_{i,3}{}^2 \right) + B_j \left(P_j^{*2} - P_{j,3}{}^2 \right)} \tag{29}$$

Since

$$P_{i,3} = P_3 \, y_{i,3} \tag{30}$$

$$P_{j,3} = P_3 \, y_{j,3} \tag{31}$$

and

$$y_{j,3} = 1 - y_{i,3} \tag{32}$$

Equation (29) can be re-written as

$$y_{i,3} = \frac{B_i \left(P_i^{*2} - P_3^2 \, y_{i,3}{}^2 \right)}{B_i \left(P_i^{*2} - P_3^2 \, y_{i,3}{}^2 \right) + B_j \left(P_j^{*2} - P_3^2 \left(1 - y_{i,3}{}^2 \right) \right)} \tag{33}$$

B_i and B_j are determined from single component experiments, P_i^* and P_j^* are determined by Margules Equation corresponding to the composition of the feed mixture, and P_3 is

obtained from the experimental permeate pressure. As a result, $y_{i,3}$ can be predicted by the Pore Flow Model. Moreover,

$$Q = Q_{liq} = Q_{vap,i} + Q_{vap,j} \tag{34}$$

Combining Equations (22), (25), (26), (27), and (34), a general equation is obtained.

$$Q = \frac{A_{mix}}{\delta}\left(P_2 - P^*\right) + \frac{B_i}{\delta}\left(P_i^{*2} - P_{i,3}{}^2\right) + \frac{B_j}{\delta}\left(P_j^{*2} - P_{j,3}{}^2\right) \tag{35}$$

Assuming that the liquid feed does not exist in the pore under extremely low P_3, the first term of Equation (35) can be neglected. It becomes

$$Q = \frac{B_i}{\delta}\left(P_i^{*2} - P_{i,3}{}^2\right) + \frac{B_j}{\delta}\left(P_j^{*2} - P_{j,3}{}^2\right) \tag{36}$$

From Equation (36), Q can be predicted by knowing B_i/δ, B_j/δ, and P_3.

4.0 Experimental Methods

4.1 Materials

4.1.1 Materials for Homogeneous Fluorosilicone Rubber Membrane

1. Fluorosilicone rubber resin (product identification: LS-420) was supplied by Dow Corning STI, Plymouth, Michigan.
2. Ethyl acetate (99.5% purity) was supplied by BDH Inc.
3. Benzoyl peroxide (97% purity) was supplied by Aldrich Chemical Company Inc.

4.1.2 Materials for Ultrafiltration Polyethersulfone Membrane

1. Polyethersulfone (product identification: PES Victrex 200p with an average molecular weight 30,000) was supplied by Imperial Chemical.
2. N-methylpyrrolidone (NMP) (99.5% purity) was supplied by Anachemia Solvents Canada, Mississauga, Ontario.
3. Polyvinylpyrrolidone (PVP with an average molecular weight 10,000) was supplied by Sigma Chemical Corp.

4.1.3 Other Materials Frequently Used in the Experiment

1. Polyethersulfone ultrafiltration membrane with a molecular weight cutoff of 55,000 (product identification: HM18) was supplied by Osmonics Co., Minnetonka, Minnesota.

2. Isopropyl alcohol (99.5% purity) was supplied by BDH Inc.

3. Glycerol (98% purity) was supplied by BDH Inc.

4. Chloroform (99% purity) was supplied by BDH Inc.

5. Polyethylene Glycol (PEG) with molecular weights 1500, 3000, 6000, 12000, 20000, and 35000 (Purum grade or > 97% purity) was supplied by Fluka Chemical Corp.

4.2 Fractionation of Polyethersulfone

One gram of PES polymer was dissolved in sixty-five grams of chloroform solvent under vigorous mechanical stirring for twelve hours. The resulting polymer/solvent mixture appeared cloudy. The polymer/solvent mixture was filtered through a filter paper (Whatman Inc., Category 2). The retentate was then washed with distilled water and dried in a vacuum oven at 100°C for 17 hours. The drying was considered complete when the weight of the polymer did not change for the last three consecutive hours. This component of polymer is hereafter called 'Undissolved PES' in contrast to PES without being subjected to chloroform treatment which is hereafter called 'Untreated PES'. The filtrate was heated to the boiling point of chloroform to remove solvent. The residue was washed with distilled water and dried in a vacuum oven at 100°C for 17 hours. The powder so collected appeared to be fine and bright white, and was most likely low molecular weight polyethersulfone, which is hereafter called 'Dissolved PES'. Untreated PES and Undissolved PES were subjected to infrared spectroscopy. All Untreated, Undissolved and Dissolved PES samples were subjected to

intrinsic viscosity measurement.

4.3 Preparation of Substrate Polyethersulfone Membrane

The substrate polyethersulfone membranes were prepared following the method reported by Lafreniére et al. (1987). The substrates made of Untreated PES are hereafter called PES membranes, whereas the substrates made of Undissolved PES are hereafter called FPES membranes. Casting solutions were prepared by loading sealed glass bottles with PES, PVP, and NMP, and placing the bottles on rolling bars in a chamber where the temperature was maintained at 50 ± 5°C. The compositions of the casting solutions prepared for PES membranes are listed in Table 4.1, and the composition of the casting solution prepared for FPES membranes was 15 wt.% of Undissolved PES, 15 wt.% of PVP, and 70 wt.% of NMP. Depending on the viscosity of the solution, 3 to 30 days were required to dissolve PES and PVP completely.

The solutions were filtered through a Teflon filter (Millipore Inc., pore size 10 μm) to eliminate any dust particles and possible invisible polymer agglomerates. The filtered solutions were then left undisturbed for a minimum of 12 hours for degassing. The solution was cast on a glass plate to a thickness of 250 μm using a casting bar in a chamber where humidity and temperature were controlled to 10 ± 1% and 23.5 ± 0.2°C, respectively. After the cast film was kept in the controlled environment for one minute, it was immersed into a gelation bath (distilled water) for 15 minutes. In the gelation bath, the solvent (NMP) was exchanged with nonsolvent (distilled water). Therefore, the PES precipitated and formed a piece of membrane. The temperature and the ionic

conductivity of the gelation bath were kept below 5°C and 5 μS/cm, respectively.

The membrane prepared was then transferred to a distilled water bath at ambient temperature for the completion of the nonsolvent-solvent exchange process. The process lasted five days with the water in the water bath changed every day. After the completion of the exchange process, the membranes were transferred to a bath of glycerol/water (30/70 by weight) mixture and kept submerged for 24 hours before they were hung to dry in the air.

Table 4.1 Compositions of casting solutions for the preparation of substrate polyethersulfone membranes.

Solutions	PES wt.%	PVP wt.%	NMP wt.%
1	15	40.5	44.5
2	15	30	55
3	20	30	50
4	15	15	70
5	15	3	82
6	15	0	85
7	20	0	80
8	20	40	40
9	25	35	40

4.4 Preparation of Homogeneous Fluorosilicone Rubber Membrane

The casting solution was prepared by dissolving fluorosilicone rubber resin (19.6 wt.%) and benzoyl peroxide (2 wt.%) in ethyl acetate (78.4 wt.%). The solvent, ethyl

acetate, was chosen from a number of solvents after preliminary experiments. The criteria for the choice of solvent were as follows, and the results of the preliminary tests are included in Appendix A.

1. The fluorosilicone rubber resin should be dissolved in the solvent completely.
2. The solvent should not produce any visual damages on ultrafiltration polyethersulfone membranes.

Benzoyl peroxide was first dissolved in ethyl acetate. Then, fluorosilicone rubber resin was introduced into the ethyl acetate/benzoyl peroxide mixture. The resulting solution was vigorously stirred by a magnetic stirrer for six hours, before being filtered through a filter paper (Whatman Inc., Category 2) to eliminate dust particles. The filtered solution was left undisturbed for 2 hours for degassing before being used in the next step.

Approximately 10 mL of the casting solution was poured slowly onto a flat Teflon sheet with a clean surface supported on a horizontal glass plate. The solution was then covered immediately by a petri-dish and left undisturbed for five minutes to allow even spreading over the Teflon sheet. After removing the petri-dish, the film was kept in an ambient environment for one minute, and then put into an oven (Fisher Scientific Ltd., Fisher Isotemp® model 418F) for solvent evaporation and cross-linking. The temperature of the oven was kept at 80 ± 1°C. After 15 hours of heating, the polymer film was slowly and carefully separated from the Teflon sheet. The polymer film (fluorosilicone rubber membrane) was ready for the permeation experiment. The thickness of the membrane was 112 ± 5 μm measured by a micrometer (Mitutoyo, No.293-761-30).

4.5 Preparation of Composite Fluorosilicone Rubber Membrane

A piece of aluminum foil was wetted on one side with 30 wt.% glycerol solution. An ultrafiltration PES membrane was placed on top of the aluminum foil, whereby the porous side of the membrane was in contact with the wetted side of the aluminum foil. Then, all the edges of the aluminum foil and the PES membrane were taped together. The substrate PES membrane/aluminum foil sheet was taped securely on a glass plate with the aluminum foil side facing to the surface of the glass plate. Then, 10 mL of the fluorosilicone rubber resin solution prepared as described in Section 4.4 was cast on top of the substrate PES membrane to a thickness of 150 μm using a casting knife in an ambient atmosphere. Thereafter, the membrane preparation procedure was the same as that of homogeneous fluorosilicone rubber membrane.

4.6 Ultrafiltration Experiment

Ultrafiltration experiment was carried out to test the pure water permeation, product rate, and solute separation performance of the PES membranes and FPES membranes. The membrane prepared in Section 4.3 was cut into circular coupons with a diameter of 4.3 ± 0.1 cm and was loaded into the ultrafiltration test cell. An ultrafiltration test cell and a continuous flow testing system are shown schematically in Figure 4.1 and Figure 4.2, respectively. Initially, the membranes were subjected to a compaction process using distilled water as feed. Compaction is a mechanical deformation of a polymeric membrane matrix that occurs in pressure-driven membrane operations. During these processes, the structure densifies and as a result the flux will decline. After relaxation

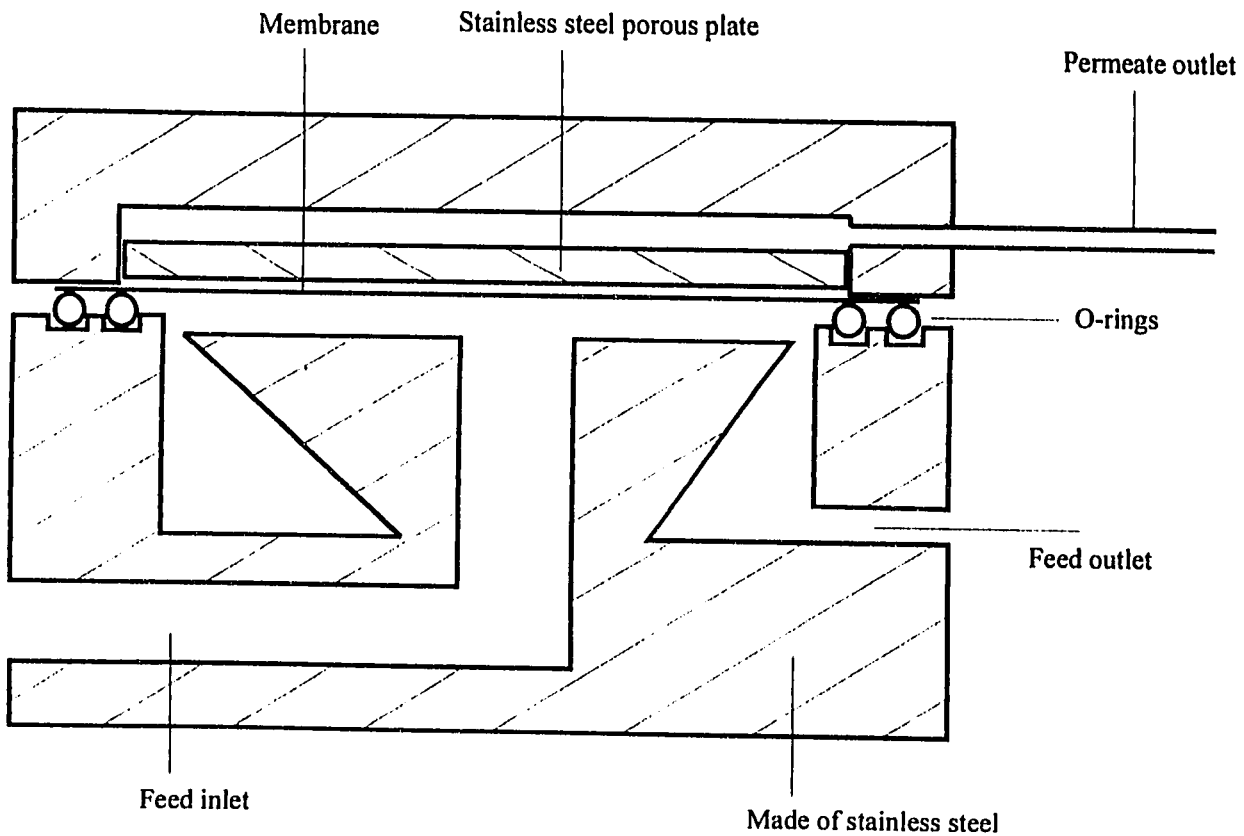

Figure 4.1 Schematic diagram for the ultrafiltration cell.

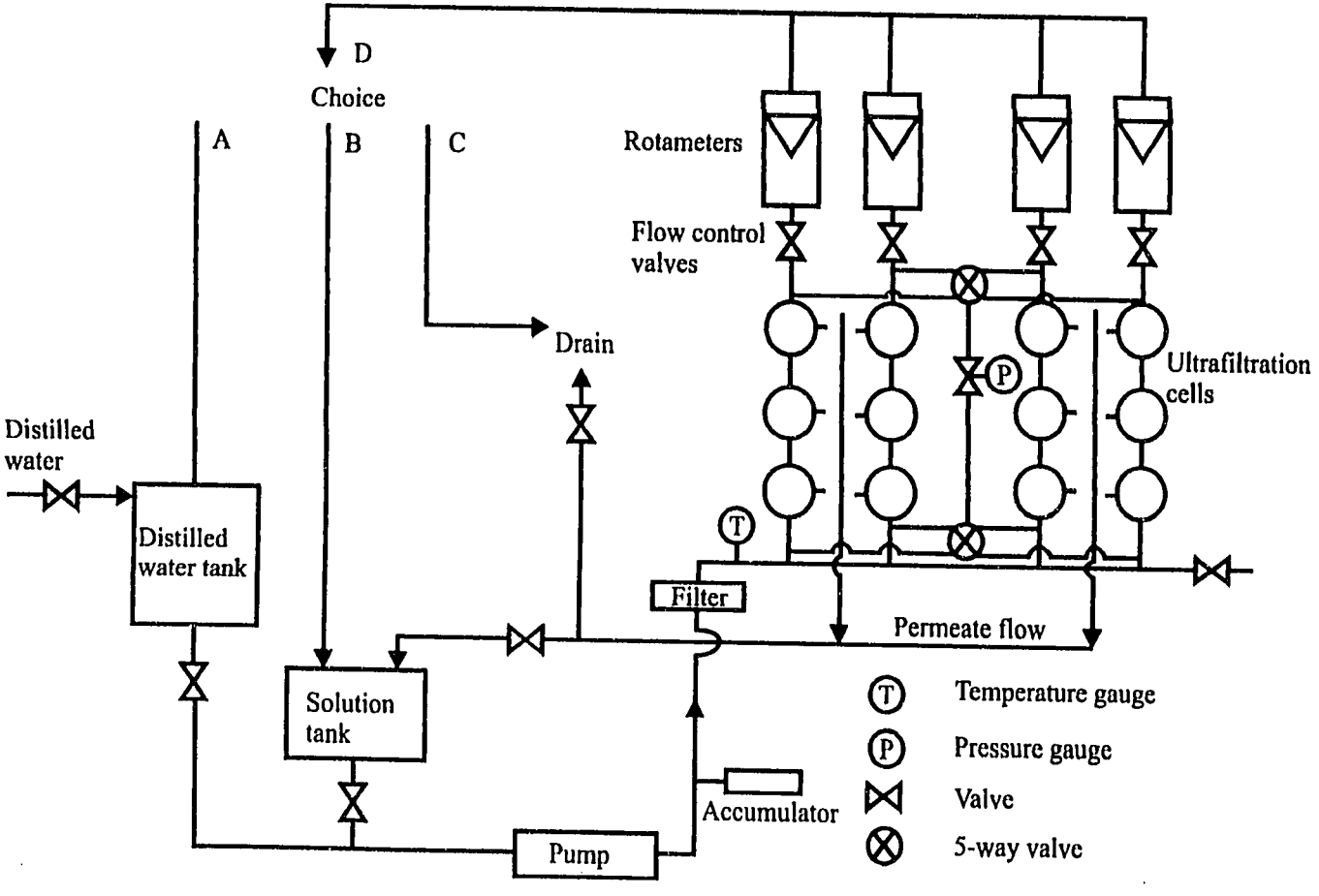

Figure 4.2 Schematic diagram for the ultrafiltration system.

(effect by reducing the pressure) the flux will return or not return to its original value depending on whether the deformation was reversible or irreversible. The compaction process was initially carried out at 70 ± 0.4 psig (483 kPa gauge pressure that was 20 psig higher than the experimental pressure for shortening the compaction time). Other operating parameters such as temperature and feed flow-rate of the feed were at room temperature (approximately 25°C) and at 0.58 ± 0.2 gallons per minute (2.2 L/min), respectively. After 672 hours, the change of permeate-flux was greatly reduced. The operating pressure was then lowered to 50 ± 0.4 psig (345 kPa gauge) with the flow-rate of the feed kept constant at 0.58 ± 0.2 gallons per minute (2.2 L/min) for another 143 hours. This compaction was considered completed at 815 hours when the consecutive pure water permeation rates did not change more than 6 wt.% in 120 hours. Then, the ultrafiltration experiment began.

The ultrafiltration experiments were conducted at the feed polyethylene glycol concentration of 200 ppm, and each test was operated for a duration of one hour before the permeate was collected for weighing and total organic carbon analysis. After each ultrafiltration test, the system was flushed with 80 liters of distilled water. Then, the system continued to operate using distilled water until the pure water permeation was approximately restored before applying another fresh feed of polyethylene glycol solution.

4.7 Pervaporation Experiment

Pervaporation experiments were carried out to test the performance of

homogeneous fluorosilicone rubber membranes and composite fluorosilicone rubber membranes. The membranes prepared as described in Sections 4.4 and 4.5 were cut into circular coupons with a diameter of 3.5 ± 0.1 cm before being placed into the pervaporation cell for testing. The pervaporation cell (a semi-batch system) and the pervaporation system are shown schematically in Figure 4.3 and Figure 4.4, respectively. Aqueous isopropyl alcohol solutions of different concentrations were used as feed solutions. After the feed solution was loaded into the pervaporation cell, vacuum was applied to the permeate side of the membrane and the permeate collected in cold trap I for six hours, during which period steady state was reached. Then, the line was switched to the cold trap II to collect a permeate sample. The feed temperature was kept at room temperature (23 ± 1°C). The permeate sample was collected for a predetermined period, usually 6 hours, before it was weighed and analyzed by gas chromatography.

4.8 Analysis

4.8.1 Total Organic Carbon Analysis

Total organic carbon analyzer (Shimadzu Corporation TOC-5050) was used to analyze the total carbon content in ultrafiltration samples. The analyzer is capable of detecting organic carbon at a level as low as 10 ppb. It is fully automated and is capable of performing a self-calibration. A few standard PEG solutions ranging from 300 ppm to 0.001 ppm were prepared for the calibration since the concentration range stated above was anticipated for the analysis.

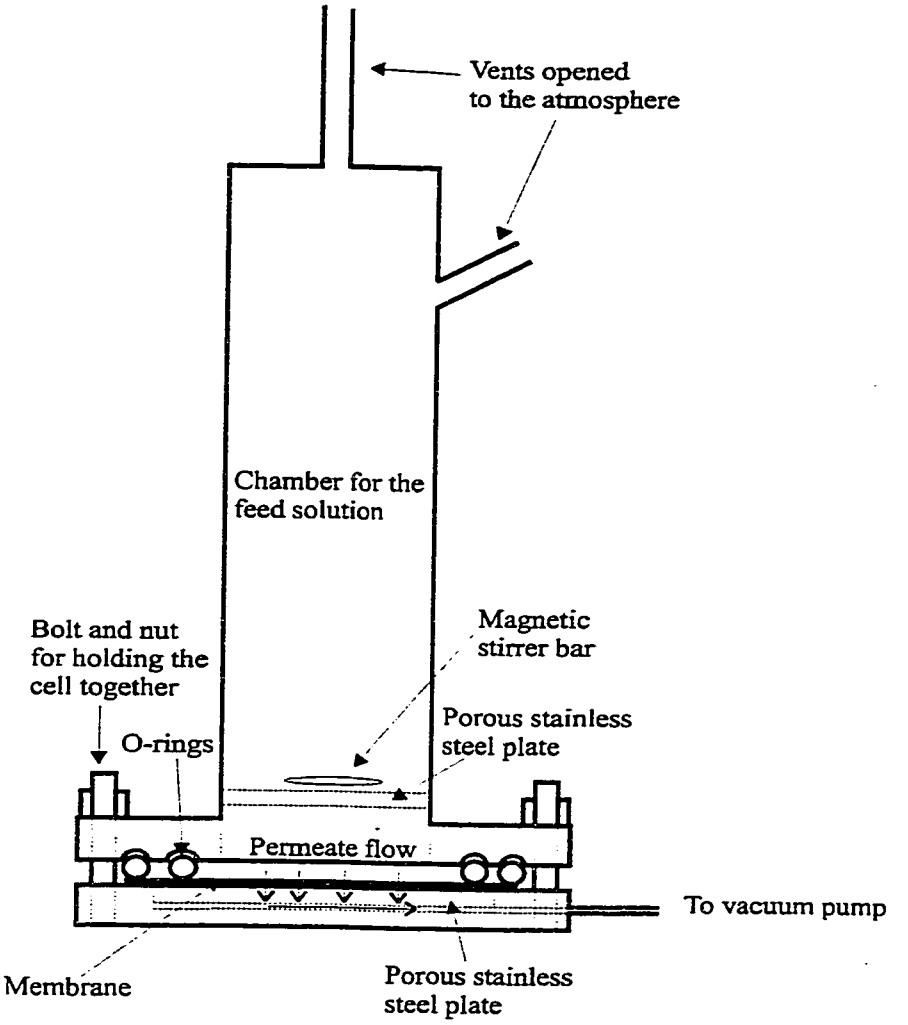

Figure 4.3 Schematic diagram for the pervaporation cell.

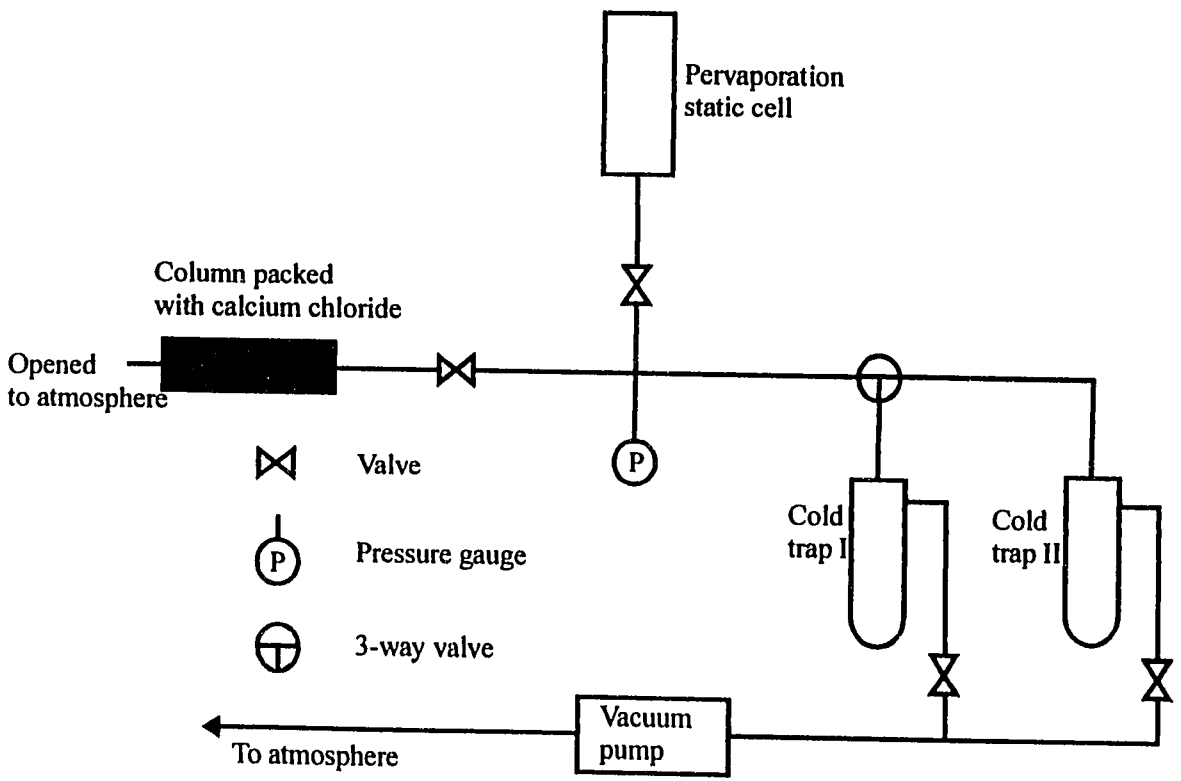

Figure 4.4 Schematic diagram for the pervaporation system.

4.8.2 Gas Chromatography

The gas chromatographic method was used to analyze the composition of samples collected from pervaporation experiments, i.e., mixtures of isopropyl alcohol and water. The column housed inside the analyzer (Varian 3400) was specified as 6' × 1.25" O.D., Porapak Q and 80/100. Each component in the sample solution was detected by a thermal conductivity detector. The temperature of the detector was set at 200°C and the temperature of the filament was set at 250°C. Helium was used as the carrier gas. The analytical result was reported by a Varian 4400 integrator with an attenuation set at 16. A calibration curve, which was generated under the conditions specified above and using aqueous isopropyl alcohol concentrations of 0, 25, 50, 75, and 100 wt.% is given in Appendix B.

4.8.3 Infrared Spectrum

Infrared spectroscopy was used to identify PES Victrex 200p and chloroform used in this work. The infrared spectrometer (Nicolet Ltd. Nicolet 520G) was purged with dry nitrogen gas for two hours prior to taking the spectrum of the sample. The sample was prepared by two techniques, the 'Multi-grind Technique' and 'KBr Window'.

The 'Multi-grind Technique' was used for powdering the polymer sample and mixing it with the KBr powder. A small metal container (volume 3 mL) was loaded with 2.5 mg of polymer, 100 mg of dry KBr powder, and a small metal ball. Then, the metal container was mounted in a shaker for one minute of vigorous shaking, followed by one minute of pounding on a table. This process was carried out five times. The metal ball

was then removed from the container, and another 300 mg of dry KBr powder was added into the metal container. The container was then shaken for one minute.

The powered mixture was used for making a 'KBr Window' using a hard press. Three tonnes (300 pounds) of force were applied to the powder mixture confined in a metal ring for 15 minutes. The KBr powder turned into a piece of clear glass-like window used for infrared spectrum analysis. KBr has extremely low absorption in the infrared range spectra.

4.8.4 Ionic Conductivity and Humidity

The ionic conductivity of a solution was measured by a conductivity meter (Cole-Parmer Model 4070), and the humidity of an environment was measured by a hygrometer (Cole-Parmer Model 37950-00). They are both equipped with a thermometer.

4.9 Intrinsic Viscosity

The intrinsic viscosity of a polymer solution was determined by a viscometer (Model no. 75L236, Cannon Co. Ltd., State College, PA) immersed in a 35°C water bath as shown in Figure 4.5. One percent by weight of polymer solution was prepared by mixing polymer and solvent at 60°C for 12 hours. The concentration of the polymer was required to be very accurate; therefore, a high precision electronic scale (accuracy of 4 decimals) was employed. The temperature of the solution was then lowered to 35°C prior to the viscosity measurement.

Three milliliters of the 1 wt.% solution was charged into the viscometer through

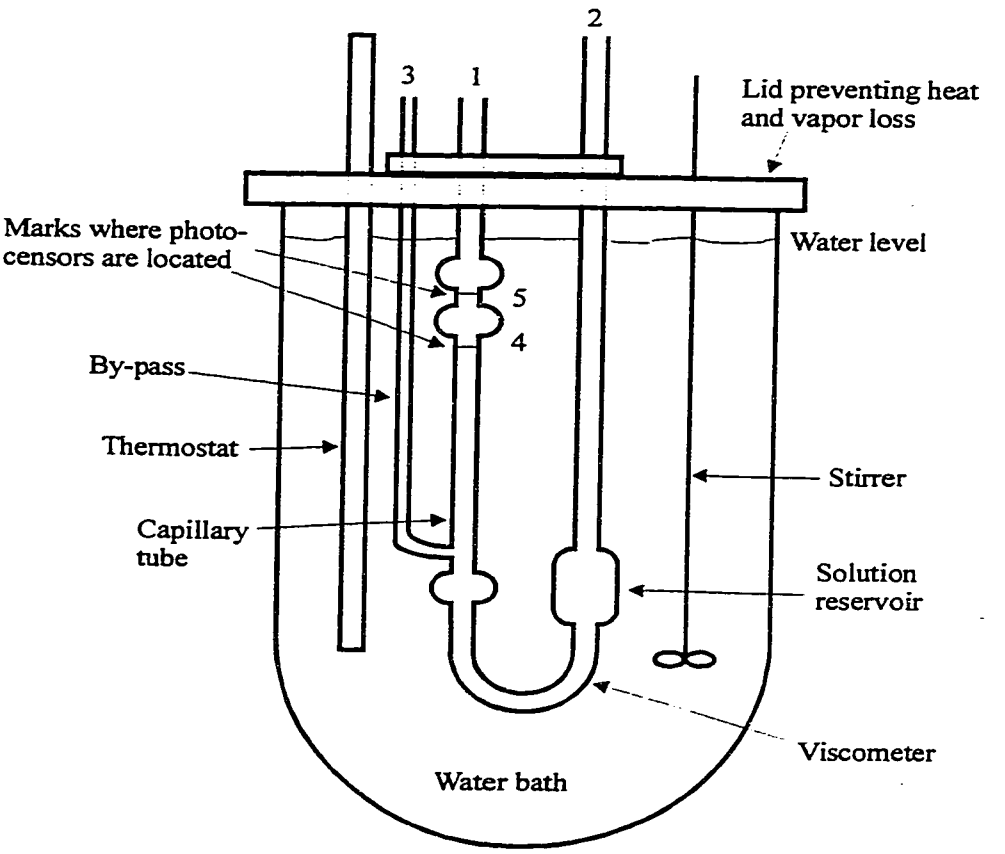

Figure 4.5 Intrinsic viscosity measurement set-up.

the inlet 2 shown in Figure 4.5. The process was very carefully performed in order to avoid the formation of any solution droplet adhering to the wall of the viscometer tube (section between inlet 2 and the solution reservoir). By blocking the inlet 3, an air-pressure was applied through the inlet 2 to force the solution in the reservoir to rise in the capillary tube until the meniscus of the solution passed Point 5. After the blockage at inlet 3 and the air-pressure applied at inlet 2 was removed, the level of the solution in the capillary tube began to fall. An automatic timer operated with a refractometer would then record the time required for the solution to fall from Point 5 to Point 4.

The polymer solution in the reservoir was diluted four times by adding approximately, 0.75 mL, 1.25 mL, 2.5 mL, and 7.5 mL of dry N-methylpyrrolidone, NMP, (at 35°C) to the reservoir. The diluting NMP and the solution were well agitated and mixed by introducing air bubbles to the reservoir. The weight of the diluting NMP added to the reservoir was precisely measured, and its volume was then calculated using the density of NMP that was known to be 1.033 g/mL at 35°C. To evaluate the intrinsic viscosity of the polymer solution, the time required for the solution after each dilution and for the pure solvent to travel from Point 5 to Point 4 was measured. The definition of the intrinsic viscosity is shown as follows:

$$\lim_{c \to 0} \frac{\eta_{sp}}{c} = [\eta] \tag{37}$$

where

$$\eta_{sp} = \frac{t - t_o}{t_o} \tag{38}$$

η_{sp} is specific viscosity, c is concentration of the polymer solution, $[\eta]$ is the intrinsic viscosity, t is time required for the polymer solution to travel from Point 5 to Point 4, and t_o is time required for the pure solvent to travel from Point 5 to Point 4. From Equation (37), it is obvious that the intrinsic viscosity of the solution can be evaluated from a plot of specific viscosity divided by concentration of the solution versus concentration of the solution by extrapolating the concentration of the solution to zero.

5.0 Results and Discussion

5.1 Infrared Spectrum and Intrinsic Viscosity of Polyethersulfone after Fractionation

As mentioned in Section 4.2, the Undissolved PES was subjected to vacuum drying for 17 hours to remove the residual chloroform. In order to verify the negligible presence of the residual chloroform, the Undissolved PES and Untreated PES were examined for their infrared spectra. The spectra may also reveal any possible chemical changes made to the polymer in the fractionation process. Their infrared spectra are shown in Appendix C. The wavenumber and the corresponding absorbance are shown in Table 5.1 for the Undissolved and Untreated PES, and chloroform. The major peaks detected for the Undissolved PES and Untreated PES were very similar to each other. The differences between both sets of spectra were not significant although there were slight shifts for some wavenumbers. They could be caused by the fact that the absorbed frequency was not a distinctive value but covered a range. Therefore, the infrared spectra were accepted as evidence that there was no detectable change in chemical structure as a result of the fractionation process. Furthermore, these two spectra were compared against the infrared spectrum of the pure chloroform (Brezinski, 1991). The set of peaks identifying chloroform was not observed in the spectra of Undissolved PES. Therefore, it was unlikely that residual chloroform was existing in the Undissolved PES. The Undissolved PES was considered chemically identical with the Untreated PES.

The intrinsic viscosities of the Untreated PES, Undissolved PES, and Dissolved

Table 5.1 Wavenumber and absorbance identifying the Undissolved PES, Untreated PES, and chloroform (Brezinski, 1991).

Undissolved PES		Untreated PES		Chloroform	
wavenumber (cm^{-1})	absorbance (%)	wavenumber (cm^{-1})	absorbance (%)	wavenumber (cm^{-1})	absorbance (%)
555.17	47	555.57	40	670	39
622.71	25	623.67	28	760	90
699.91	35	700.59	33	1220	63
719.21	37	718.35	34	3040	18
757.71	16	756.81	20		
796.41	22	795.27	25		
830.19	32.5	833.74	31		
868.79	33	869.24	32		
1008.7	31	1008.3	30		
1071.4	36	1070.4	31.5		
1100.4	42	1103	38		
1148.6	44	1147.4	39		
1240.3	42	1239.1	39.5		
1298.2	35	1298.3	33.5		
1327.1	35	1327.8	34		
1409.2	23	1410.7	26.5		
1486.4	41	1487.6	39		
1578	40	1579.3	38		
1631.6	19	1629.6	23		

PES were also examined for comparison purposes. Figures 5.1, 5.2, and 5.3 show η_{sp}/c vs c plots. After extrapolating the regression line to the y-intercept, the measured intrinsic viscosities for the Untreated PES, Undissolved PES, and Dissolved PES were 4.32×10^{-5} m^3/kg, 4.33×10^{-5} m^3/kg, and 1.21×10^{-5} m^3/kg, respectively. Mark-Houwink-Sakurada Equation (Brandrup and Immergut, 1989), that directly relates the intrinsic viscosity to the molecular weight of polymer is shown below:

$$[\eta] = K\, M^a \tag{33}$$

where K and a are called Mark-Houwink constants. Since the intrinsic viscosity of the Dissolved PES was much lower than those of untreated and Undissolved PES, the Dissolved PES was considered to be a low molecular weight fraction that was extracted from the Untreated PES.

5.2 Ultrafiltration Test for Substrate Polyethersulfone Membranes Made of Treated and Undissolved PES

5.2.1 Separation of Polyethylene Glycol Solution and Permeation Flux

As mentioned in Section 4.3, the PES and FPES membranes underwent a five-day nonsolvent-solvent exchange process. The completion of nonsolvent-solvent exchange process was examined by monitoring the total organic carbon level in the bath every day. The process was considered completed when the total organic carbon level went down to the same level as distilled water. Table 5.2 shows the total organic carbon content for

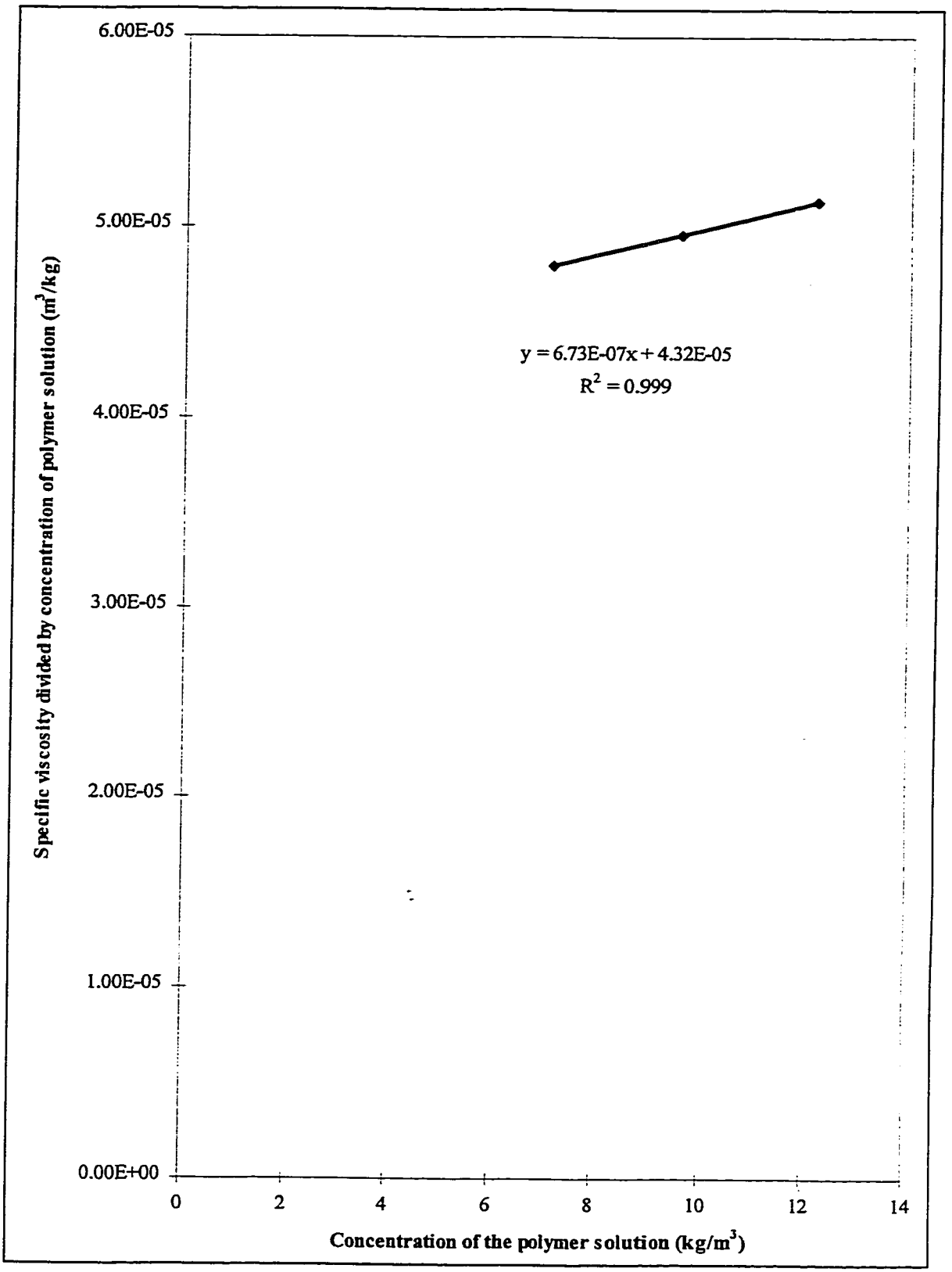

Figure 5.1 Determination of intrinsic viscosity for the Untreated PES.

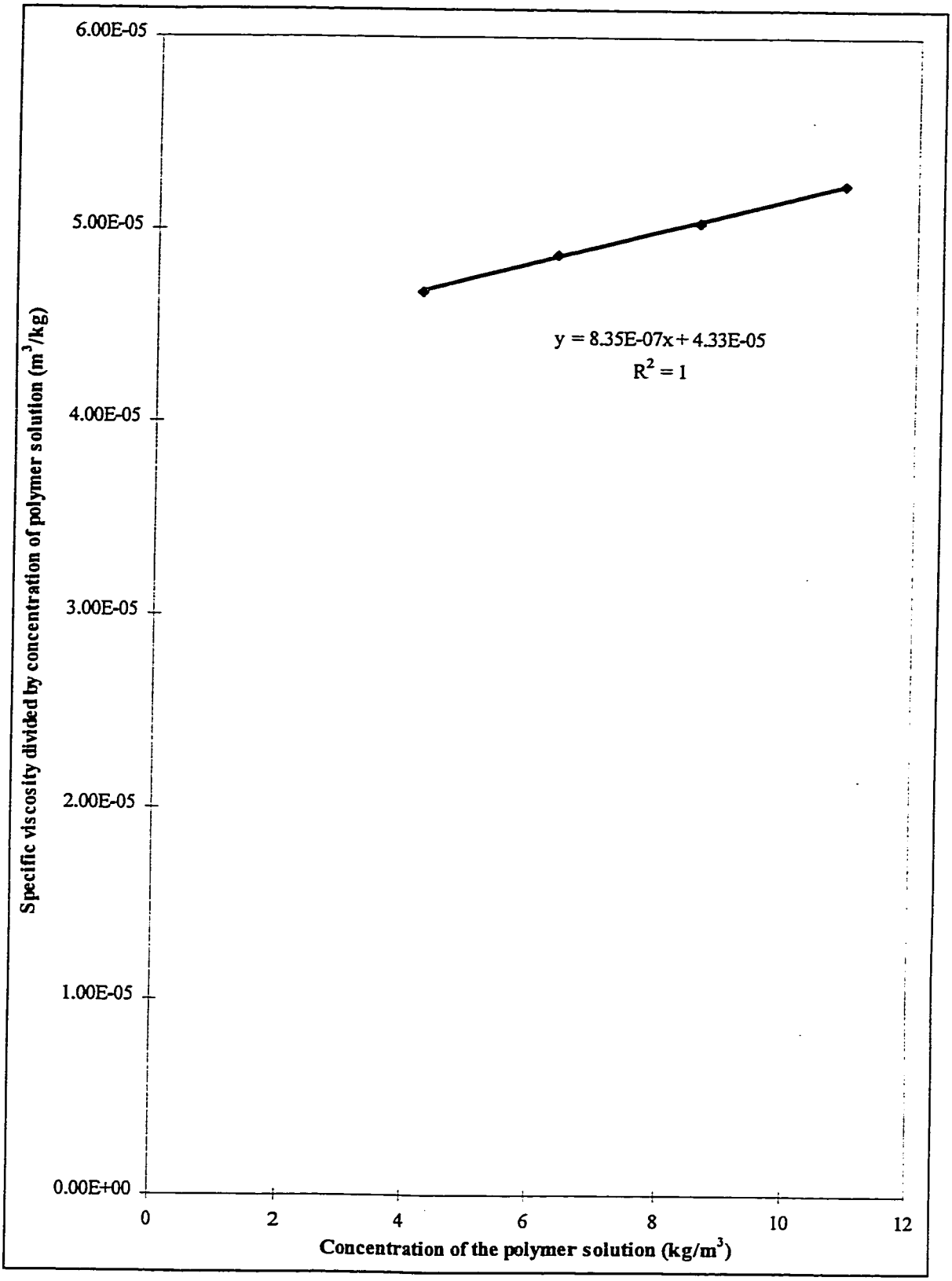

Figure 5.2 Determination of intrinsic viscosity for the Undissolved PES.

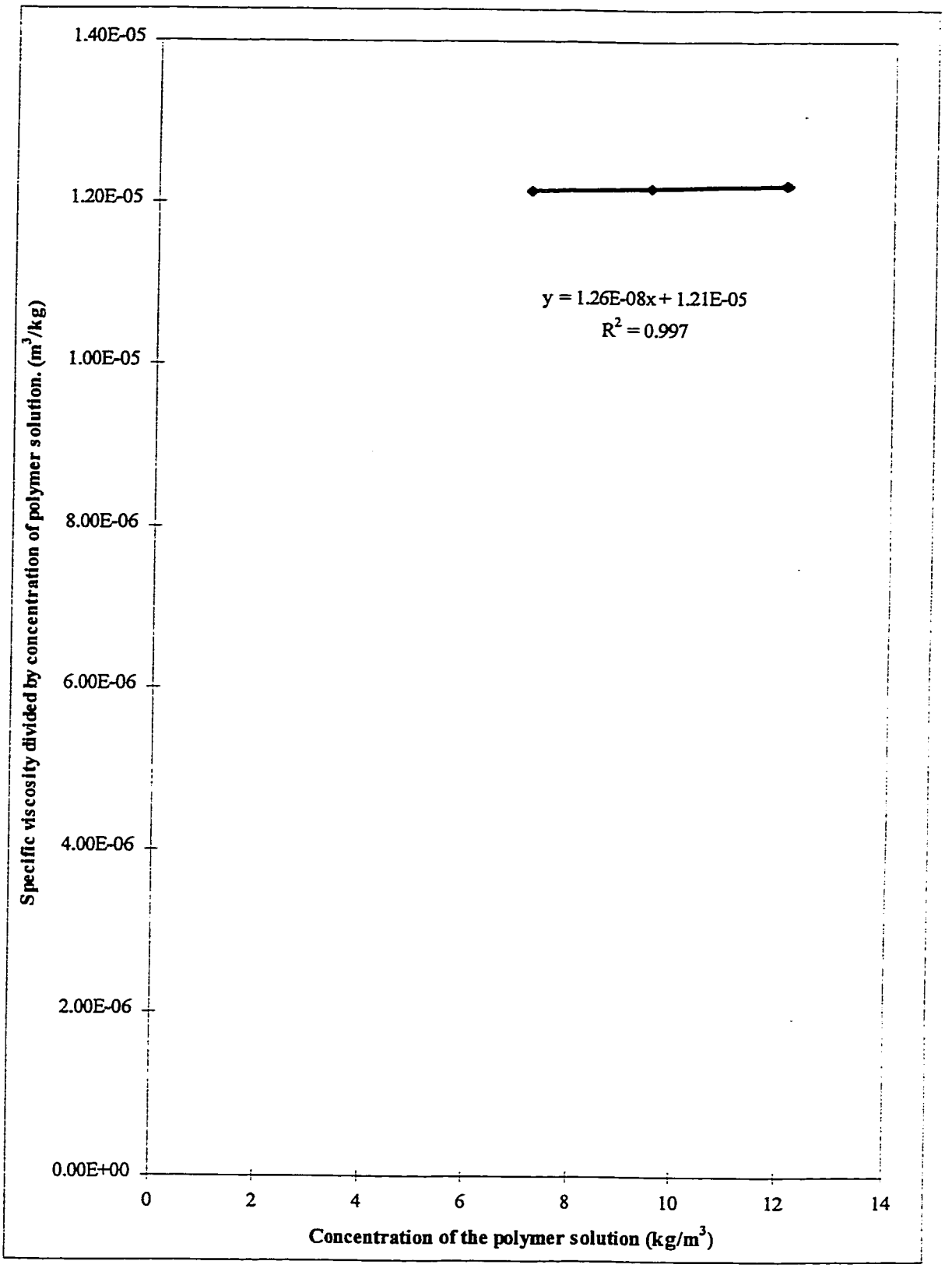

Figure 5.3 Determination of intrinsic viscosity for the Dissolved PES.

two separate water baths. It shows that the nonsolvent-solvent exchange was completed in three days. Therefore, a five-day period was considered sufficient for the nonsolvent-solvent exchange process to be completed. The membranes were tested for ultrafiltration immediately after the fifth day of the nonsolvent-solvent exchange process. There were four PES membranes and five FPES membranes tested for ultrafiltration. The average pure water permeation flux (PWP) of PES membranes and of FPES membranes during the compaction stage is shown in Figure 5.4. The pure water permeation flux for individual membrane, average pure water permeation flux and the standard deviations for both types of membranes are shown in Appendix D.

Table 5.2 Total organic carbon level of two separate water baths during the nonsolvent-solvent exchange process.

Day	Total organic carbon in the water bath		Total organic carbon in distilled water (ppm)
	Bath 1 (ppm)	Bath 2 (ppm)	
1	106.7	157.9	0.014
2	10.75	11.64	0.014
3	0.014	0.014	0.014
4	0.014	0.014	0.014
5	0.014	0.014	0.014

Figure 5.4 shows that the permeation flux decreased rapidly as the membranes were compacted. However, the rate of decrease in flux diminished gradually after the

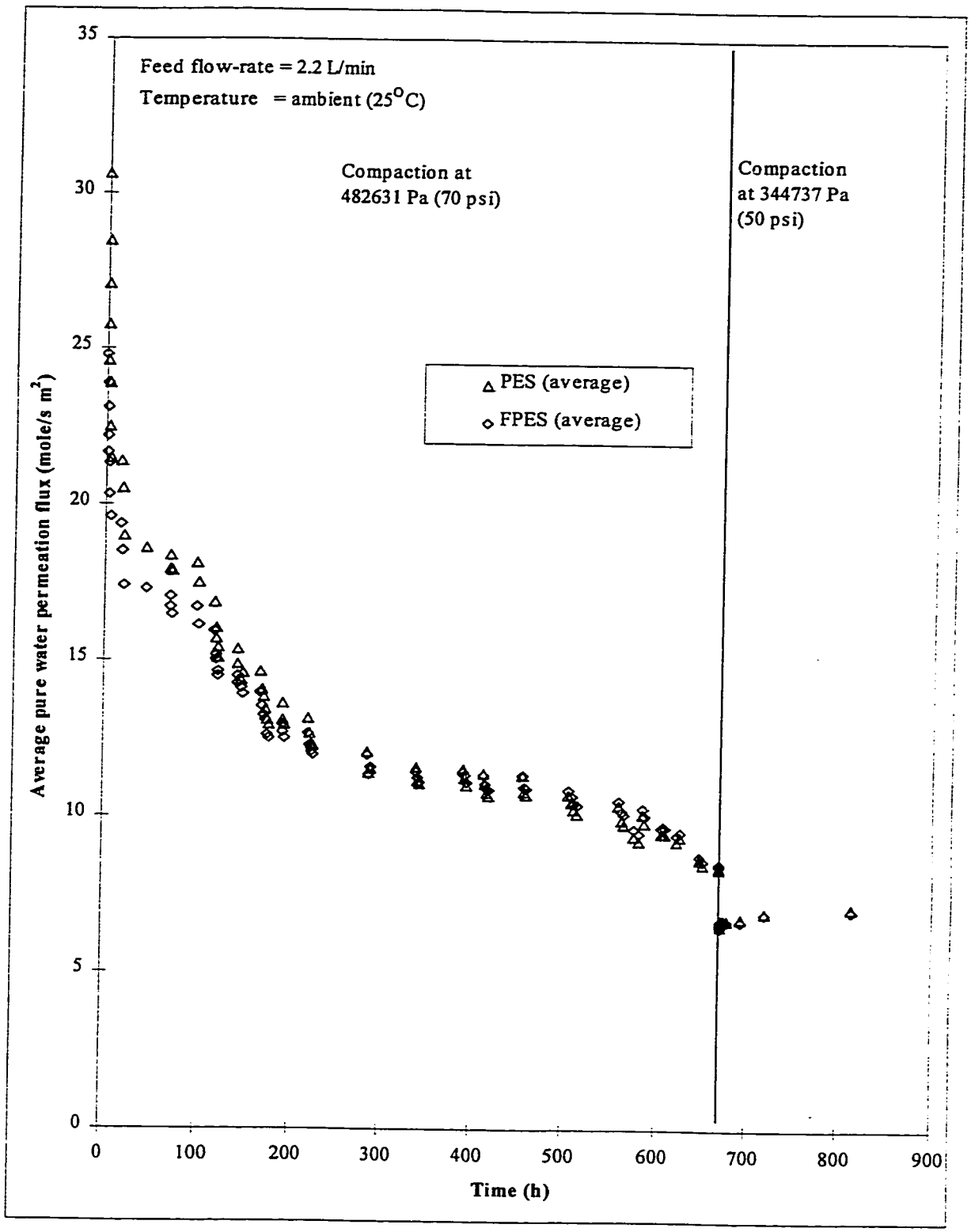

Figure 5.4 **Change in average pure water permeation flux during the compaction stage.**

initial five hours. This was possibly due to the slow and reluctant change of the membrane matrix configuration. After 200 hours, the permeation flux of both types of membranes showed very little difference from each other.

After 672 hours of compaction at 482631 Pa (70 psig), the operating pressure was lowered to 344737 Pa (50 psi), and the compaction was continued for another 143 hours. The pure water permeation flux reduced rapidly because of the decreased pressure. In the second stage of compaction, the permeation flux was more steady than in the first stage. The change of the flux was less than 6% over 120 hours. Even a slight increase in flux was detected at the beginning of the second stage. This might be due to the 'relaxation' of the polymer matrix of the membranes. After 815 hours of continuous compaction, the permeation flux attained a 'stable' value, the feed was switched from pure water to PEG solution and an ultrafiltration experiment was started. The average pure water permeation flux of PES membrane was 7.18 mole/s m^2 with a standard deviation of 0.61 after 815 hours of compaction under pure water. For FPES membranes, the average pure water permeation flux was 7.07 mole/s m^2 with a standard deviation of 0.16 after 815 hours of compaction under pure water. The smaller standard deviation of FPES membrane may be indicative of more uniform morphology of the latter membranes as compared with the PES membrane.

The average product rates of PEG solutions for both types of membrane are shown in Figure 5.5. Product rates for individual membranes are shown in Appendix E. The average permeate flux through the PES membranes was always higher than the fluxes though the FPES membranes. This was due to the average thickness of FPES

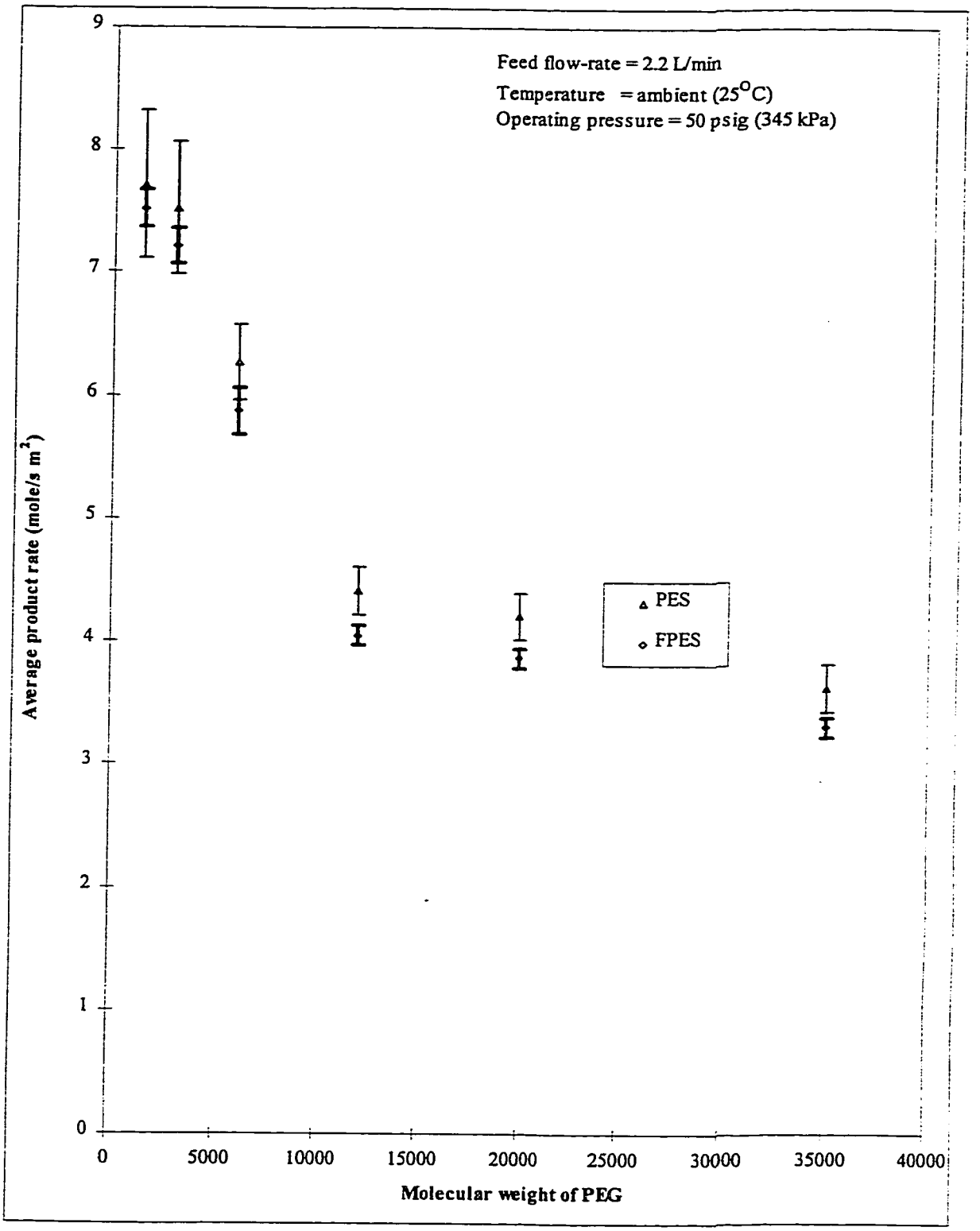

Figure 5.5 **Average product rates of PEG solutions (200 ppm PEG/water mixture) for PES and FPES membranes.**

membrane thicker than the average thickness of PES membrane. Figure 5.5 also shows that the permeate flux decreased as the PEG molecular weight increased. As PEG molecular weight increases, the bulkiness of the molecule increases, resulting in more friction between PES molecule and membrane pore wall. The flow of solvent water is also prevented by the slowly moving PEG molecule. Furthermore, one can also expect that separation of PEG solute with a higher molecular weight would be better than PEG solute of lower molecular weight. Figure 5.6 shows the average solute rejection curve for the PEG solutions. The data for individual membranes are shown in Appendix F. Appendix G contains the numerical values of average product rates, and average solute rejections, and their standard deviations for each PEG solution. Again, the standard deviations for the FPES membranes are smaller than those for the PES membranes.

Throughout the PEG solution separation experiment, pure water permeation flux was monitored before each PEG solution test. The flux fluctuated between ± 12% and ± 9% for PES and FPES membranes, respectively. This fluctuation could be caused by the slight change of the operating temperature. However, the pure water permeation flux was considered stable. Data for the individual membranes are shown in Appendix H.

5.2.2 Average Pore Sizes of Substrate Polyethersulfone Membranes

A log-normal probability plot of PEG-solute rejection versus Einstein-Stokes Radius PEG solute is shown in Figure 5.7. The geometric mean pore sizes and standard deviations determined by the method described in the theoretical section are shown in Table 5.3. Interestingly, both the mean pore size and the standard deviation are within the

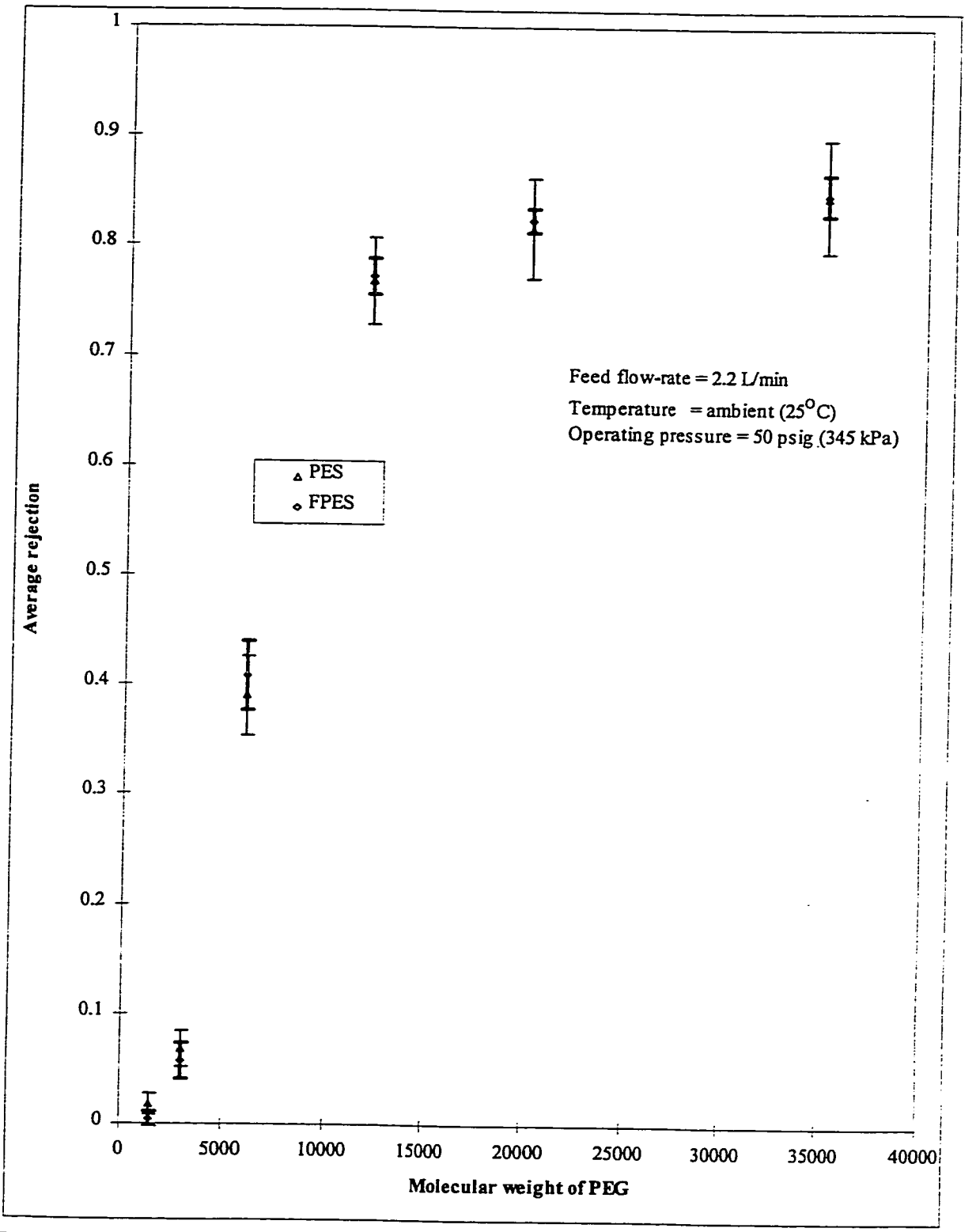

Figure 5.6 **Average solute rejection of PEG solutions (200 ppm PEG/water mixture) for PES and FPES membranes .**

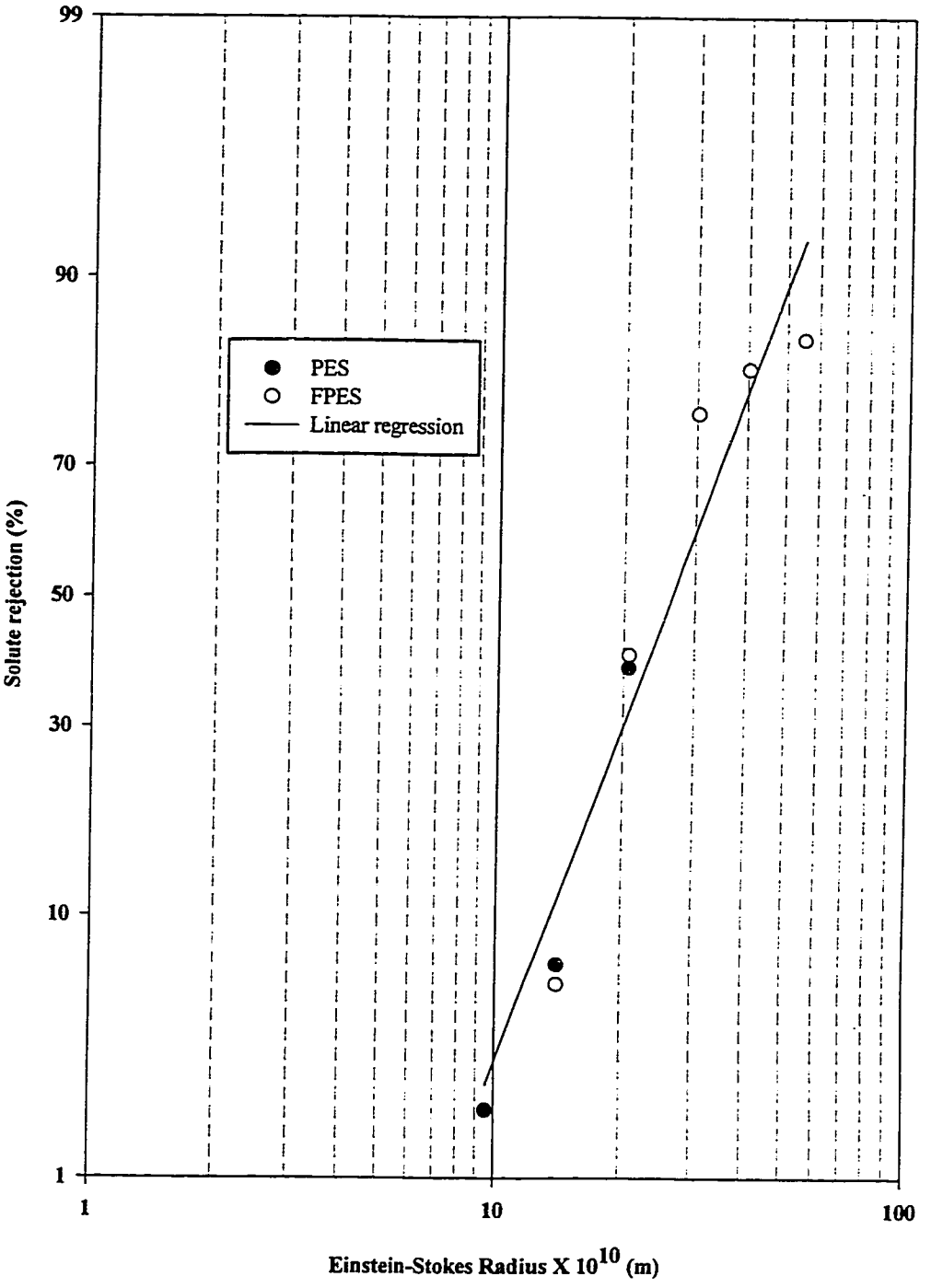

Figure 5.7 Pore size estimation for substrate polyethersulfone membranes.

range given by Michaels (1980) for several ultrafiltration membranes. According to Michaels, the mean pore radius varied between 17 and 34 Å, while the geometric standard deviation varied between 1.2 and 1.7.

Table 5.3 Geometric mean pore size and standard deviation for PES and FPES membranes.

Membrane	Geometric mean pore size (Å)	Geometric standard deviation
PES and FPES	26.82	1.71

Since the rejection data shown in Figure 5.6 from both PES and FPES membranes differ insignificantly from each other, the geometric mean pore size and standard deviation for both types of membrane are the same. Thus, the fractionation did not show effect on the pore size and the pore distribution. However, during the fractionation process, it was found that only 7.6 wt.% of Untreated PES was extracted into chloroform solvent as low molecular weight fraction. Supposing that chloroform had reached its solubility limit in the above experiment, a larger quantity of chloroform could have extracted a larger amount of low molecular weight PES. Then, the effect of fractionation on the pore size and pore size distribution of the ultrafiltration membrane might have been observed.

5.3 Pervaporation Test for Homogeneous Fluorosilicone Rubber Membrane

5.3.1 Homogeneous Fluorosilicone Rubber Membrane Tested with Pure Isopropyl Alcohol and Distilled Water

Homogeneous fluorosilicone rubber membranes were tested at various downstream pressures. The plot of permeate flux versus down stream pressure is shown in Figures 5.8 for the pervaporation of pure isopropyl alcohol and water. The results are also tabulated in Appendix I. At low downstream pressure (160 Pa), the water flux was higher than the isopropyl alcohol flux. However, the water flux decreased more rapidly than the isopropyl alcohol flux as the downstream pressure increased. When downstream pressure increases, the driving force (the pressure difference between saturated vapor pressure and downstream pressure) for permeation decreases. Although the driving force for water is always smaller than the one for isopropyl alcohol, the resistance force for water is smaller than the one for isopropyl alcohol. Therefore, in low downstream pressure the driving force for water permeation is sufficiently high to produce water permeation that is higher than isopropyl alcohol permeation. However, the driving force for water permeation diminishes more rapidly than the one for isopropyl alcohol permeation. As a result, the water flux decreased more rapidly than the isopropyl alcohol flux. The water flux became lower than the isopropyl alcohol flux at approximately 800 Pa. There are some discrepancies between the predictions of pore model and the experimental data. They may be due to the assumptions made in the model. In the vicinity of downstream pressure higher than saturated pressure, the predictions differ

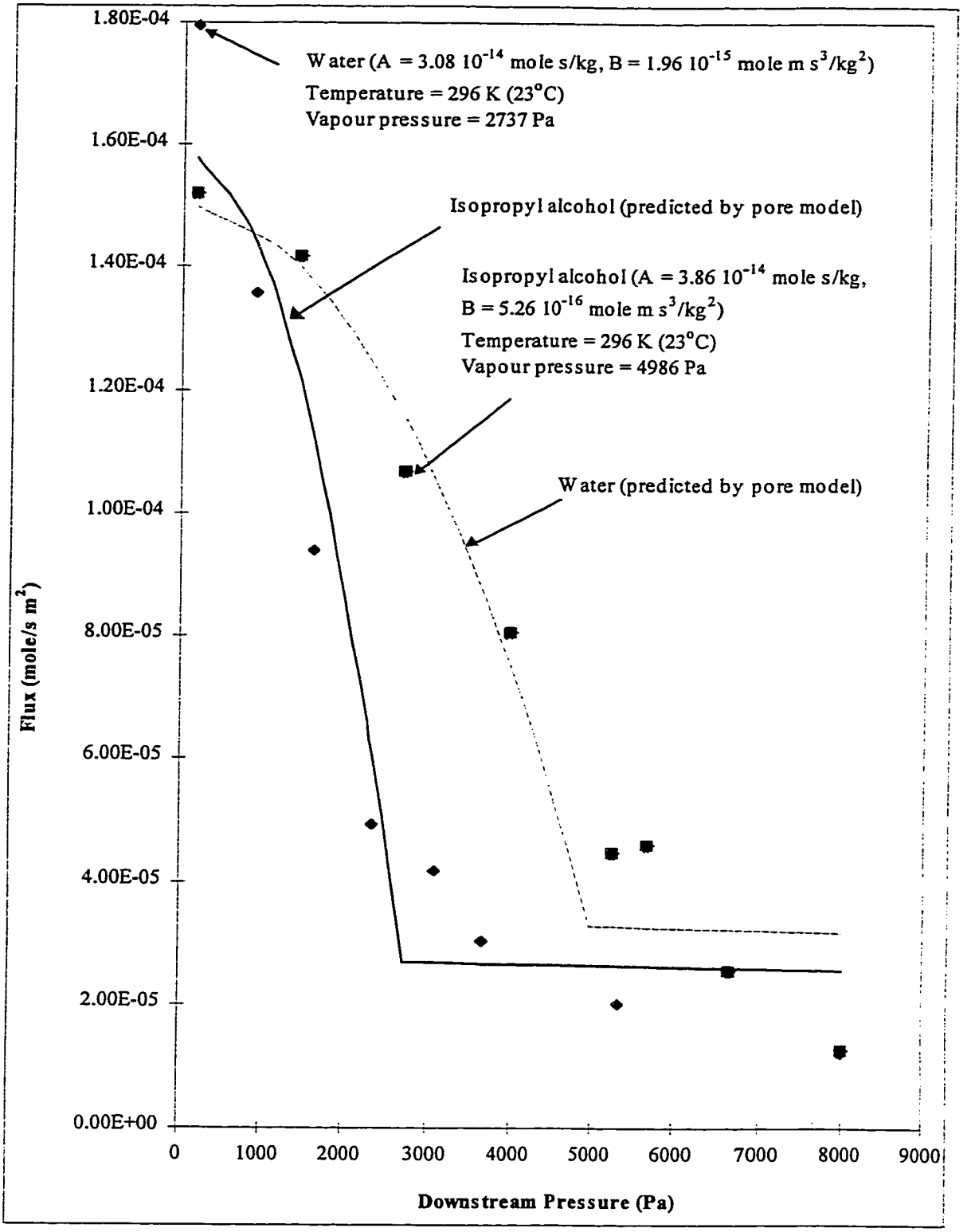

Figure 5.8 Pemeate flux versus downstream pressure for homogeneous fluorosilicone rubber membrane.

greatly from the experimental data. The decrease of flux of experimental data is much faster than of the prediction. This shows that the flux of liquid permeate is not linearly proportional to the driving force.

From Figure 5.8, A/δ and B/δ were determined for the water (liquid)-fluorosilicone rubber-water (vapor) and isopropyl alcohol (liquid)-fluorosilicone rubber-isopropyl alcohol (vapor) systems. For the former system, A/δ is equal to 2.75×10^{-10} mole s/kg m, and B/δ is equal to 1.75×10^{-11} mole s^3/kg^2. For the latter system, A/δ is equal to 3.44×10^{-10} mole s/kg m, and B/δ is equal to 4.7×10^{-12} mole s^3/kg^2. Since the thickness of the homogeneous fluorosilicone rubber membrane was measured to be 112 μm as mentioned in Section 4.4, A and B for both systems could be calculated. Their values are shown in Figure 5.8. The saturated vapor pressure of water at the vapor-liquid-equilibrium state occurred at 2737 Pa, whereas the saturated vapor pressure of isopropyl alcohol at the vapor-liquid-equilibrium state occurred at 4986 Pa.

5.3.2 Homogeneous Fluorosilicone Rubber Membrane Tested with Isopropyl Alcohol/Water Mixture

Homogeneous fluorosilicone rubber membranes were tested for various water concentrations in feed with downstream pressure maintained at 160 Pa (1.2 torrs), at which the pure water flux differed greatly from the pure isopropyl alcohol flux and the minimum downstream pressure could be achieved. A plot of permeate composition versus feed composition is shown in Figure 5.9. Similarly, permeate flux is plotted versus feed composition Figure 5.10. Their numerical values are tabulated in Appendix J.

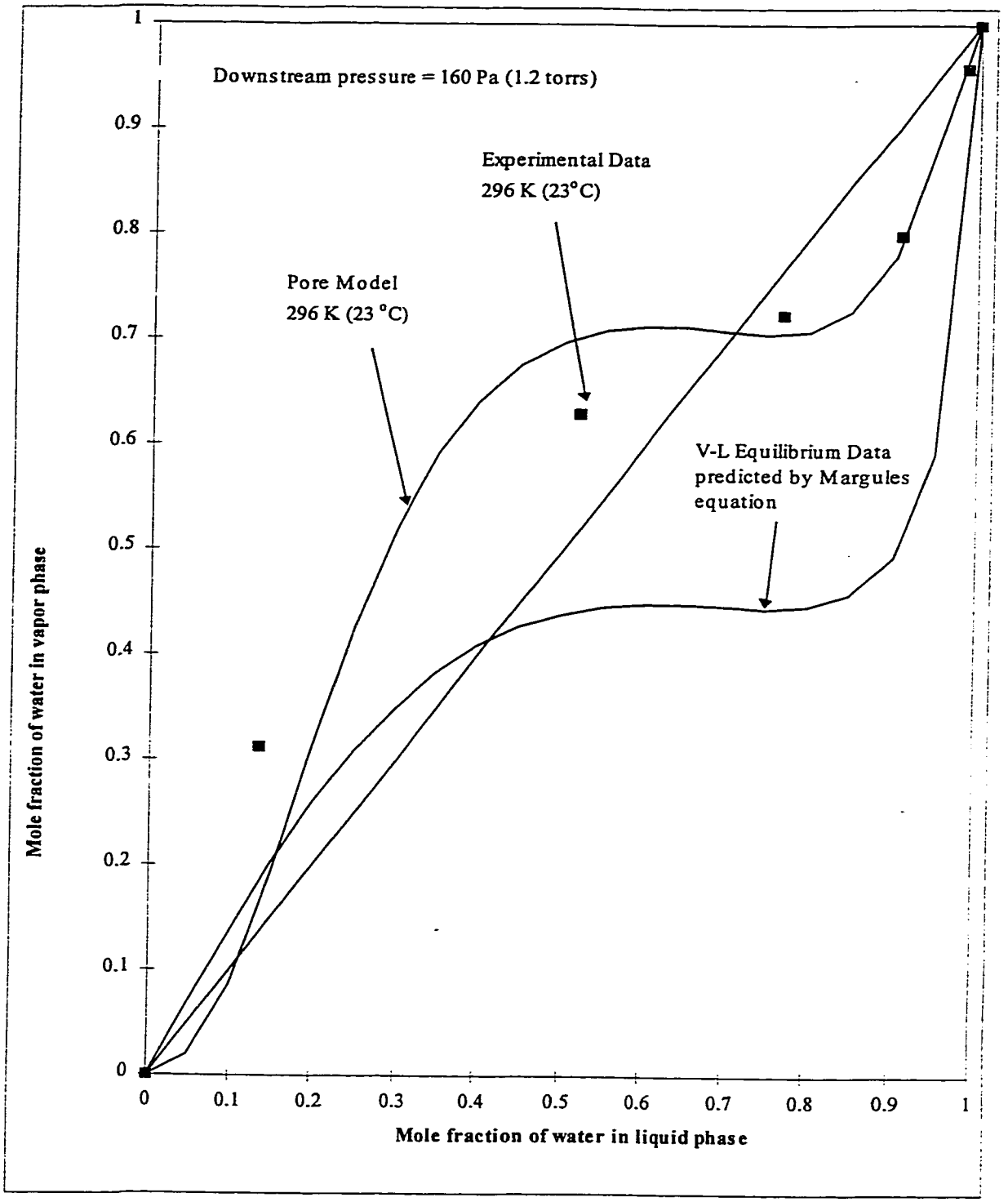

Figure 5.9 **Mole fraction of water in the liquid phase and vapor phase for homogeneous fluorosilicone rubber membrane and liquid-vapor equilibrium.**

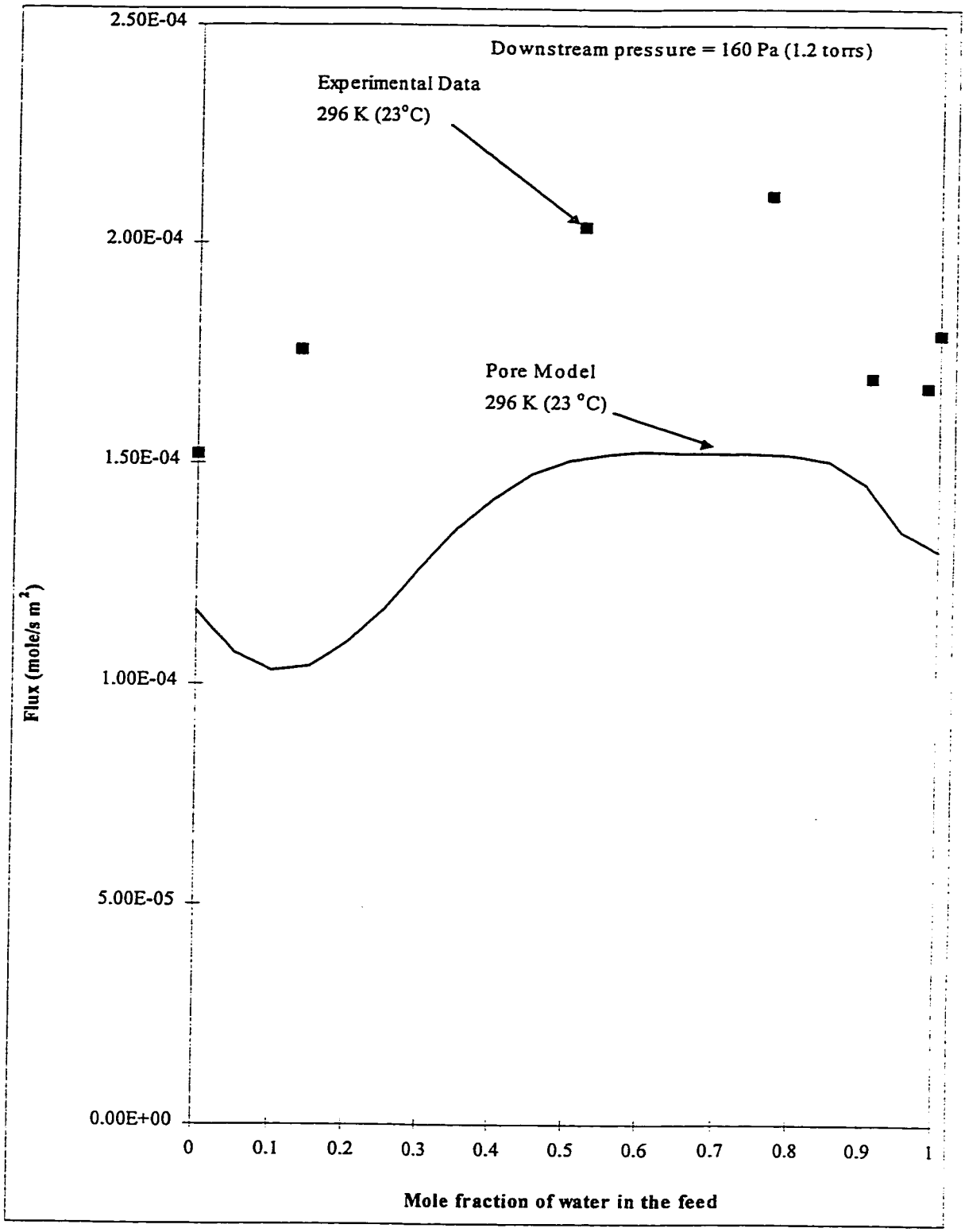

Figure 5.10 Permeate flux versus mole fraction of water in the feed for homogeneous fluorosilicone rubber membrane.

According to the experimental data in Figure 5.9, a change of selectivity was observed at 70 mole% of water in the feed. The selectivity of the membrane changed from water-selective to isopropyl alcohol-selective. According to the vapor-liquid equilibrium predicted by Margules Equation, the azeotropic point is at approximately 41 mole% of water in the feed. Therefore, introduction of a membrane phase (membrane made of polar material, fluorosilicone rubber) enhanced the water composition in the vapor phase to some extent. With this observation, one can assume that a membrane made of a more polar material would further increase the composition of water in the vapor phase. The example of such a material is polyvinyl alcohol.

Figure 5.9 shows that the predicted permeate composition using the Pore Model differed from the experimental data. However, the predictions can be made closer to the experimental data if the assumption that feed liquid does not penetrate into the membrane phase is removed. It should be noted that the model predicts that there are two change-of-selection points. One is at 76 mole% of water in the feed. It is deviated by approximately 7 mole% from the experimental value. The other point is at 9 mole% of water in the feed. It would be interesting to confirm the existence of the second change-of-selectivity point experimentally. According to the prediction of the pore model, the homogeneous fluorosilicone rubber membrane is isopropyl alcohol-selective when the water content in the feed is low or high. When the water content is high, in other words isopropyl alcohol content is low, vapor-liquid equilibrium predicts lower water contents (higher isopropyl alcohol contents) in vapor than pervaporation. Therefore, pervaporation process using fluorosilicone rubber does not seem to be a method preferable to distillation. On the

other hand, it may be used as a system to enhance water enrichment in the vapor phase, if the water content in the feed is between 9 mole% and 76 mole%.

In Figure 5.10, the permeate flux predicted by the pore model is compared with the experimental data. The predicted values are consistently lower than experimental values but follow the trend of experimental data. This may be simply caused by an assumption made in the model that the liquid-vapor phase boundary is at the pore inlet. Therefore, the term corresponding to the liquid phase transport in the membrane pore was dropped from the permeate flux prediction. Also, the effective thickness of the membrane would have been increased in this assumption. Therefore, a lower permeation flux prediction can be anticipated. In the same figure, it is also observed that the predicted permeate flux goes through a minimum and maximum at lower and higher change-of-selectivity points, respectively. As for experimental data, the flux showed a maximum at the higher change-of-selectivity point. It would be interesting to confirm the presence of a minimum flux which corresponds to the lower change-of-selectivity point.

5.4 Pervaporation Test for Composite Fluorosilicone Rubber Membrane

All composite fluorosilicone rubber membranes were tested under the same experimental condition. Downstream pressure, water content in the feed, and temperature were 160 Pa, 5 wt% (15 mole%), and ambient temperature, respectively. Also, a term called separation factor (α) used hereafter is required to be defined at this point.

$$\alpha = \frac{\dfrac{\text{mole fraction of water in the permeate}}{\text{mole fraction of isopropyl alcohol in the permeate}}}{\dfrac{\text{mole fraction of water in the feed}}{\text{mole fraction of isopropyl alcohol in the feed}}} \qquad (39)$$

5.4.1 Composite Fluorosilicone Rubber Membranes Protected by Aluminum Foil during the Heat-Treatment Process.

As described in Sections 4.4 and 4.5, the preparation of composite membranes involves heat treatment of the coated fluorosilicone rubber layer at 80°C. At this temperature, the substrate layer (PES membrane) was also subjected to this 'high' temperature. The pores of the substrate PES membrane may undergo shrinkage as reported by Lang (1993). Therefore, a simple method was developed in this study to protect the substrate layer from shrinkage during heat treatment.

The polyethersulfone membrane (HM18) supplied by Osmonics was used in this section of experiment. It was preserved in glycerol when received from the company. Therefore, it did not undergo the glycerol/water mixture treatment as other membranes which were laboratory-prepared. It is known that glycerol or glycerol/water mixture, when filling the pore, prevents the membrane pore from collapsing when the membrane is dried at room temperature (Singh et al. 1997). In order to minimize the evaporation of glycerol during the heat treatment, the glycerol filled PES membrane was sandwiched between a coated fluorosilicone rubber layer and a piece of aluminum foil, as illustrated schematically in Figure 5.11. Glycerol is confined between two layers without being

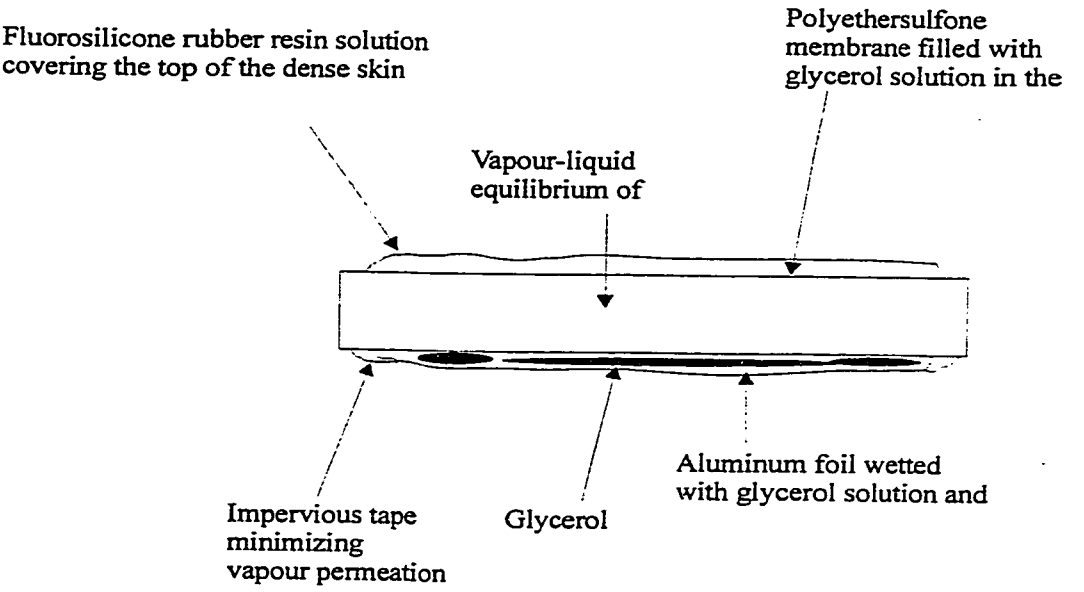

Figure 5.11 Composite membrane protected by an aluminum foil during heat treatment.

evaporated into the atmosphere. The aluminum foil was removed before the composite membrane was tested for pervaporation.

Four composite membranes protected by an aluminum foil and four membranes without aluminum foil were tested by the pervaporation experiment for comparison. Table 5.4 shows the results of this test. The average flux of protected membranes was approximately 22% higher than the unprotected membranes, whereas separation factor of the former membranes were 213% lower than the latter. Although the separation factor of the unprotected membrane is much higher than the separation factor of the protected membrane, the standard deviation for the separation factor of the unprotected one is enormously large. Therefore, the high separation factor is not reliable, and all composite membranes made thereafter were protected by aluminum foil.

Table 5.4 Pervaporation results for the protected and unprotected composite fluorosilicone rubber membrane in the heat-treatment.

Fluorosilicone rubber composite membrane	Flux (mole/s m^2)		Separation factor	
	Average	Standard deviation	Average	Standard deviation
Protected by aluminum foil	0.0022	0.00015	4.77	0.95
Unprotected by aluminum foil	0.0018	0.00019	14.95	7.18

Operating temperature = 23 °C, downstream pressure = 160 Pa (1.2 torrs), and feed = isopropyl alcohol/water mixture.

5.4.2 Composite Fluorosilicone Rubber Membrane Made of PES Membrane or FPES Membrane.

Two types of substrate polyethersulfone were used in making composite fluorosilicone rubber membranes. One was made of FPES membranes and the other of PES membranes. These two types of substrate membranes were further coated with a fluorosilicone rubber layer and the resulting composite membranes were tested for pervaporation. The results obtained from the pervaporation test are shown in Table 5.5.

The permeate flux for both types of membranes are very close to each other. However, the average separation factor for the composite membrane made of FPES membrane was slightly higher than that of PES membrane. This difference did not seem to be very significant. However, the standard deviations of both flux and separation factor are much lower for composite membranes made of the FPES membrane. This may again indicate that the FPES membranes are morphologically more uniform than the PES membranes.

5.4.3 Effect of Pore Size of Substrate Membrane on Composite Fluorosilicone Rubber Membrane

The PES membranes were made of casting solutions with various compositions as listed in Table 4.1 of Section 4.3. These substrate membranes were used to make composite fluorosilicone rubber membranes as described in Section 4.5. The mean pore sizes were determined by Lafrenière et al. (1987) as they are listed in Table 5.6. Lafrenière reported two types of pore size distributions for each PES membrane.

Table 5.5 Results of pervaporation test for composite fluorosilicone rubber membranes made of PES membrane and FPES membrane.

Composite fluorosilicone rubber membrane	Flux (mole/s m^2)		Separation factor	
	Average	Standard deviation	Average	Standard deviation
FPES membrane as substrate	0.0013	0.00022	8.3	0.41
PES membrane as substrate	0.0014	0.00057	6.82	1.9

Operating temperature = 23 °C, downstream pressure = 160 Pa (1.2 torrs), and feed = isopropyl alcohol/water mixture.

Table 5.6 shows the mean pore sizes of the substrate membranes. In the first column of the table, membrane codes are given. The first letter 'C' means composite membrane, whereas the following digit corresponds to the solution code given in Table 4.1. Table 5.6 also includes the pervaporation results. When examining the experimental data of homogeneous fluorosilicone rubber membrane, the separation factor was calculated to be 2.93 for the feed with the composition of water 0.15 mole%. When examining all the experimental separation factors of all composite membranes shown in Table 5.6, they are all more than 2.93 except C1 membrane. This indicates an effect of the porous substrate membrane on the overall performance of the composite membrane. The effect becomes the strongest when the pore size on the substrate membrane is as small as 5.05 μm. Separation factor of 16.77 was achieved for this membranes. Although the data are

scattered considerably, one may notice that C9, C8, C7, C6, and C1 behaves consistently - permeate flux increases as the mean pore size increases, and the separation factor decreases as the mean pore size increases. On the other hand, C5, C4, C3, and C2 do not follow the expected tendency. Their separation factors form a local maximum whereas their fluxes form a local minimum. This phenomenon is difficult to be explained as there is not sufficient research conducted to study these behaviours. Therefore, further study on this behaviour is recommended.

Table 5.6 Results of pervaporation test on composite fluorosilicone rubber.

Composite fluorosilicone rubber membrane	Pore radius (Lafrenière et al.,1987) (nm)	Separation factor (%)	Flux (mole/s m^2)
C9	5.05	16.77	0.00046
C8	9.4	4.99	0.00076
C7	11.8	4.41	0.00118
C6	12.4	4.03	0.00170
C5	12.8	5.49	0.00121
C4	13	8.30	0.00131
C3	13.2	6.21	0.00111
C2	14.3	5.90	0.00127
C1	16.8	2.82	0.00254

Operating temperature = 23 °C, downstream pressure = 160 Pa (1.2 torrs), and feed = isopropyl alcohol/water mixture.

6.0 Conclusions

1. The low molecular weight PES (Victrex 200p) was successfully fractionated from the high molecular weight PES by chloroform.
2. Judging from the rejection curve analysis, geometric mean pore size and geometric standard deviation for the PES and FPES membrane were the same.
3. Increase in the uniformity of molecular weight of polyethersulfone polymer exhibited positive effects on the performance of the ultrafiltration polyethersulfone membrane.
4. At low downstream pressure, homogeneous fluorosilicone rubber membrane enhanced the water concentration in the vapor phase when compared with the liquid-vapor equilibrium predicted by the Margules Equation for the water-isopropyl alcohol system.
5. In general, pervaporation experiments using the composite fluorosilicone rubber membranes revealed that permeate flux increased as the pore size of the substrate membrane increased, whereas the separation factor decreased as the pore size of the substrate membrane increased.
6. The homogeneous fluorosilicone rubber membrane and composite fluorosilicone rubber membrane are of low commercial value because of their relatively low separation factor and permeate flux.
7. Increase in the uniformity of molecular weight of polyethersulfone polymer exhibited positive effects on the performance of the composite fluorosilicone rubber membrane.

7.0 Recommendations

1. Uniformity of the molecular weight of polyethersulfone and its effect on the performance of membranes are suggested to be further studied in other membrane separation processes.
2. The water-selectivity is anticipated to be enhanced if fluorosilicone rubber is replaced by a more polar material such as polyvinyl alcohol.
3. The homogeneous fluorosilicone rubber membrane should be tested for different feed compositions and at different downstream pressures.
4. Similarly, the composite fluorosilicone rubber membrane should be tested for different feed compositions and at different downstream pressures.

8.0 References

Bai, J., A. E. Fouda, T. Matsuura and J. D. Hazlett, "A Study on the Preparation and Performance of Polydimethylsiloxane-Coated Polyetherimide Membrane in Pervaporation", J. Appl. Polym. Sci., **48**, 999-1008 (1993).

Binning, R. C. and F. E. James, "Permeation. A New Commercial Separation Tool", Pet. Eng., **30**(6), c14-c15 (1958).

Binning, R. C., R. J. Lee, J. F. Jennings and E. C. Martin, "Separation of Liquid Mixtures by Permeation", Ind. Eng. Chem., **53**, 45-48 (1961).

Binning, R. C., J. F. Jenning and E. C. Martin, "Removal of Water from Organic Chemicals", US Patent 3,035,060 (1962).

Blume, I., J. G. Wijmans and R. W. Baker, "The Separation of Dissolved Organics from Water by Pervaporation", J. Membrane Sci., **49**(3), 253-286 (1990).

Brezinski, D. R. (eds.), Infrared Spectroscopy Atlas Working Committee, "An Infrared Spectroscopy Atlas for the Coatings Industry", 4th ed., Vol.1, Federation of Societies for Coatings Technology, Blue Bell, Pennsylvania (1991).

Brandrup, J., E.H. Immergut, Polymer Handbook (3rd ed.), New York: Wiley (1989).

Brun, J. P., C. Larchet, G. Bulvestre and B. Auclari, "Sorption and Pervaporation of Dilute Aqueous Solutions of Organic Compounds through Polymer Membranes", J. Membr. Sci., **25**(1), 55-100 (1985a).

Brun, J. P., C. Larchet, R. Melet and G. Bulvestre, "Modeling of the Pervaporation of Binary Mixtures through Moderately Swelling, Non-reacting Membranes", J. Membr. Sci., **23**(3), 257-283 (1985b).

Chen, Y., A. Fouda and T. Matsuura, "A Study on Dry Cellulose Acetate Membrane for the Separation of Carbon Dioxide/Methane Gas Mixtures", Advances in Reverse Osmosis and Ultrafiltration, eds. Matsuura, T., and Sourirajan, S., National Research Council of Canada, Ottawa, Ontario, 259-278 (1989).

Deng, S., S. Sourirajan and T. Matsuura, "A Study of Polydimethylsiloxane/Aromatic Polyamide Laminated Membranes for Separation of Acetic Acid/Water Mixtures by Pervaporation Process", Sep. Sci. Technol., **29**(9), 1209-1216 (1994).

Doong, S. J., W. S. Ho and R. P. Matondrea, "Prediction of Flux and Selectivity in Pervaporation through a Membrane", J. Membr. Sci., **107**(1-2), 129-146 (1995).

Fels, M. and R. Y. M. Huang, "Theoretical Interpretation of the Effect of Mixture Composition on Separation of Liquids in Polymers", J. Macromol. Sci. Phys., **5**(1), 89-109 (1971).

Franken, A. C. M., M. H. V. Mulder and C. A. Smolders, "Pervaporation Process Using a Thermal Gradient as the Driving Force", J. Membr. Sci., **53**(1-2), 127-141 (1990).

Gilliland, E. R., R. F. Baddown and J. L. Russell, "Rates of Flow through Microporous Solids", AIChEJ., **4**, 90-96 (1958).

Goncalves, M. D. C., D. Windmoller, N. D. M. Erismann and F. Galembeck, "Pressure Driven Pervaporation", Sep. Sci. Technol., **25**(9-10), 1079-1085 (1990).

Greenlaw, F. W., W. D. Prince, R. A. Shelden and E. V. Thompson, "Dependence of Diffusive Permeation Rates on Upstream and Downstream Pressures. I. Single Component Permeant", J. Membr. Sci., **2**(2), 141-151 (1977).

Gudernatsch, W., Th. Menzel and H. Strathmann, "Influence of Composite Membrane Structure on Pervaporation", J. Membr. Sci., **61**, 19-30 (1991).

Heintz, A. and W. Stephan, "A Generalized Solution Diffusion Model of the Pervaporation Process through Composite Membranes. 1. Prediction of Mixture Solubilities in the Dense Active Layer Using the Uniquac Model", J. Membr. Sci., **89**(1-2), 143-151 (1994a).

Heintz, A. and W. Stephan, "A Generalized Solution Diffusion Model of the Pervaporation Process through Composite Membranes. 2. Concentration Polarization, Coupled Diffusion and the Influence of the Porous Support Layer", J. Membr. Sci., **89**(1-2), 153-169 (1994b).

Heinzelmann, W., "Fabrication Methods for Pervaporation Membranes", Proc. of 5th Int. Conf. Pervaporation Process in Chem. Ind., Englewood, NJ, 22-30 (1991).

Heisler, E. G., A. S. Hunter, J. Siciliano and R. H. Treadway, "Solute and Temperature Effects in the Pervaporation of Aqueous Alcoholic Solutions", Science, **124**, 77-78 (1956).

Hsieh, F. -H., T. Matsuura and S. Sourirajan, "Reverse Osmosis Separations of Polyethylene Glycols in Dilute Aqueous Solutions Using Porous Cellulose Acetate Membranes", J. Appl. Polym. Sci., **23**(2), 561-573 (1979).

Hsieh, F. -H., T. Matsuura and S. Sourirajan, "Analysis of Osmosis Data for System Polyethylene Glycol-Water-Cellulose Acetate Membrane at Low Operating Pressures", Ind. Eng. Chem. Proc. Des. Develop., **18**(3), 414-423 (1979).

Huang, R. Y. M., "Pervaporation Membrane Separation Process", Elsevier, Amsterdam, 270-271 (1991).

Huang, R. Y. M. and X. Feng, "Dehydration of Isopropanol by Pervaporation Using Aromatic Polyetherimide Membranes", Sep. Sci. Technol., **28**(11-12), 2035-2048 (1993a).

Huang, R. Y. M. and X. Feng, "Resistance Model Approach to Asymmetric Polyetherimide Membranes for Pervaporation of Isopropanol/Water Mixtures", J. Membr. Sci., **84**(1-2), 15-27 (1993b).

Huang, R. Y. M. and J. W. Rhim, "Prediction of Pervaporation Separation Characteristics for Methanol-Pentane-Nylon-6-Poly(acrylic acid) Blended Membrane System", J. Membr. Sci., **71**(3), 211-220 (1992).

Jian, K. and P. N. Pintauro, "Integral Asymmetric Poly(vinylidene Fluoride)(PVDF) Pervaporation Membranes", J. Membr. Sci., **85**(3), 301-309 (1993).

Kataoka, T., T. Tsura, S. Nakao and S. Kimura, "Memrane Transport Properties of Pervaporation and Vapor Permeation in Ethanol-Water System Using Polyacrylonitrile and Cellulose Acetate Membranes", J. Chem. Eng. Jpn., **24**(3), 334-339 (1991a).

Kataoka, T., T. Tsura, S. Nakao and S. Kimura, "Permeation Equations Developed for Prediction of Membrane Performance in Pervaporation, Vapor Permeation and Reverse Osmosis Based on the Solution-Diffusion Model", J. Chem. Eng. Jpn., **24**(3), 326-333 (1991a).

Kesting, R. E., "Synthetic Membranes: A Structure Perspective", ed. 2nd, Wiley, New York (1985).

Kober, P. A., "Pervaporation, Perstillation, and Percrystallization", J. Am. Chem. Soc., **39**, 944-950 (1917).

Laboratoire de Recherches et de Contrôle du Caoutchouc (LRCC), "Premiere Partie: Elastomeres de Fluorosilicone", Rapport Technique No. 142 (1983).

Lai, J. -Y., Y. -H. Chu, S. -L. Huang and Y. -L. Yin, "Separation of Water Alcohol Mixtures by Pervaporation through Asymmetric Nylon 4 Membrane", J. Appl. Polym. Sci., **53**(8), 999-1009 (1994).

Lang, K., "Synthesis and Properties of Thin-Film Polyvinyl Alcohol Composite Membranes", A Thesis for the Degree of Master of Applied Science, The Department of Chemical Engineering, The University of Ottawa, Ottawa, Ontario, Canada (1993).

Lafrenière, L. Y., F. D. F. Talbot, T. Matsuura and S. Sourirajan, "Effect of Polyvinylpyrrolidone Additive on the Performance of Polyethersulfone Ultrafiltration Membranes", Ind. Eng. Chem. Res., **26**(11), 2385-2389 (1987).

Lee, C. H., "Theory of Reverse Osmosis and Some Other Membrane Permeation Operations", J. Appl. Polym. Sci., **19**, 83-95 (1975).

Lee, Y. M., E. M. Shin and K. S. Yang, "Pervaporation Separation of Water-Ethanol through Modified Chitosan Membranes. 1. Chitosan-Acetic Acid and -Metal Ion Complex Membranes", Polym. (Korea), **15**, 182 (1991a).

Lee, Y. M., E. M. Shin and S. T. Noh, "Pervaporation Separation of Water-Ethanol through Modified Chitosan Membranes. 2. Carboxylmethyl, Carboxylethyl, Cyanoethyl, and Amidoxime Chitosan membranes", Angew. Makromol. Chem., **192**, 169-181 (1991b).

Lee, Y. M., E. M. Shin and C. N. Chung, "Pervaporation Separation of Water-Ethanol through Modified Chitosan membranes. 3. Sulfonated Chitosan membranes", Polym. (Korea), **15**(4), 497-500 (1991c).

Lee, Y. M. and E. M. Shin, "Pervaporation Separation of Water-Ethanol through Modified Chitosan Membranes. 4. Phosphorylated Chitosan Membrane", J. Membr. Sci., **64**(1-2), 145-152 (1991d).

Lee, Y. M., S. Y. Nam and J. H. Kim, "Pervaporation of Water-Ethanol through Polyvinyl Alcohol/Chitosan Blend Membrane", Polym. Bull., **29**(3-4), 423-429 (1992).

Lee, Y. M., "Modified Chitosan Membranes for Pervaporation", Desalination, **90**(1-3), 277-290 (1993).

Li, S. G., G. H. Koops, M. H. V. Mulder, T. van den Boomgaard and C. A. Smolders, "Wet Spinning of Integrally Skinned Hollow Fiber Membranes by a Modified Dual-Bath Coagulation Method Using a Triple Orifice Spinneret", J. Membr. Sci., **94**, 329-340 (1994).

Loeb, S. and S. Sourirajan, "Sea Water Determination by Means of a Semi Permeable Membrane", University of California, Los Angeles, Report No. 60-60 (1960).

Lu, X. and C. Gao, "Research on Polyethersulfone, Polyarylsulphone and Polyetheretherketone with Cardo Membranes", Desalination, **96**, 155-161 (1994).

Maeda, Y., M. Tsuyumoto, H. Karakane and H. Tsugaya, "Separation of Water-Acetic Acid Mixtures by Pervaporation through Aromatic Polymer Membranes", Proc. of 5th Int. Conf., Pervaporation Processes in Chem. Ind., Englewood, NJ, 31-44 (1991).

Matsuura, T. and S. Sourirajan, "Preferential Sorption Capillary Flow Mechanism and Surface Force-Model-Applicability to Different Membrane Separation Processes", eds. Matsuura, T. and Sourirajan, S., Advances in Reverse Osmosis and Ultrafiltration, National Research Council of Canada, Ottawa, Ontario, 139-176 (1989).

Mandelkern, L. and P. J. Flory, Chem. Phys., **20**, 212-214 (1952).

Michaels, A. S., "Analysis and Prediction of Sieving Curves for Ultrafiltration Membranes: A Universal Correlation ?", Sep. Sci. Technology, **15**(16), 1305-1322 (1980).

Mulder, M. H. V. and C. A. Smolders, "On the Mechanism of Separation of Ethanol/Water Mixtures by Pervaporation. I. Calculations of concentration Profiles", J. Membr. Sci., **17**(3), 289-307 (1984).

Mulder, M. H. V., T. Franken and C. A. Smolders, "Preferential Sorption versus Preferential Permeability in Pervaporation", J. Membr. Sci., **22**(2-3), 155-173 (1985a).

Mulder, M. H. V., A. C. M. Franken and C. A. Smolders, "On the Mechanism of Separation of Ethanol/Water Mixtures by Pervaporation. II. Experimental Concentration Profiles", J. Membr. Sci., **23**(1), 41-58 (1985b).

Mulder, M. H. V. and C. A. Smolders, "Pervaporation, Solubility Aspects of the Solution-Diffusion Model", Sep. Puri. Method., **15**(1), 1-19 (1986).

Neel, J., "Introduction to Pervaporation. In Pervaporation Membrane Separation Process", ed. Huang, R. Y. M., Elsevier, Amsterdam, 1-109 (1991).

Okada, T. and T. Matsuura, "A New Transport Model for Pervaporation", J. Membr. Sci., **59**(2), 133-150 (1991).

Okada, T., M. Yoshikawa and T. Matsuura, "A Study on the Pervaporation of Ethanol-Water Mixtures on the Basis of Pore Flow Model", J. Membr. Sci., **59**(2), 152-168 (1991).

Okada, T. and T. Matsuura, "Predictabilty of Transport-Equations for Pervaporation on the Basis of Pore-Flow Mechanism", J. Membr. Sci., **70**, 163-175 (1992).

Osawa, Z., "Kobunshi no Hikari Rekka to Anteika", CMC, Tokyo (1986).

Rhim, J. W. and R. Y. M. Huang, "On the Prediction of Separation Factor and Permeability in the Separation of Binary Mixtures by Pervaporation", J. Membr. Sci., **46**(2-3), 335-348 (1989).

Rhim, J. W. and R. Y. M. Huang,, "Prediction of Pervaporation Separation Characteristics for the Ethanol-Water-Nylon-4-Membrane System", J. Membr. Sci., **70**(2-3), 105-118 (1992).

Singh, S., T. Matsuura and P. Ramamurthy, "Treatment of Excess White-Water and Coating Plant Effluent by Modified Polyethersulfone Ultrafiltration Membrane", Proceeding of TAPPI Environmental Conference, 881-898 (1997).

Sourirajan, S. and T. Matsuura, "Reverse Osmosis/Ultrafiltration Process Fundamentals", National Research Council of Canada, Chapter 4, Ottawa, Ontario (1985).

Tam, C. M., M. Dal-Cin and M. D. Guiver, "Polysulfone membranes. IV. Performance Evaluation of Radel A/PVP membranes", J. Membr. Sci., **78**(1-2), 123-134 (1993).

Tanihara, N., K. Tanaka, H. Kita, K. Okamoto, A. Nakamura, Y. Kusuki and K. Nakagawa, "Vapor Permeation Separation of Water-Ethanol Mixtures by Asymmetric Polyimide Hollow Fiber Membrane Modules", J. Chem. Eng. Jpn., **25**(4), 388-396 (1992).

Timashev, S. F., V. V. Valuev, R. R. Salem and A. G. Strugatshaga, "Pervaporation Induced by Electric Current", J. Membr. Sci., **91**(3), 249-258 (1994).

Wijmans, J. G. and C. A. Smolders, "Preparation of Asymmetric membranes by Phase Inversion Process", eds. Bungay, P. M., Lonsdale, H. K., de Pinho, M. N. and Reidal, D., Synthetic Membranes: Science, Engineering and Application, Amsterdam, 39-56 (1986).

Wijmans, J. G. and R. W. Baker, "The Solution-Diffusion Model: A Review", J. Membr. Sci., **107**(1-2), 1-21 (1995).

Yanagishita, H., C. Maejina, D. Kitamoto and T. Nakane, "Preparation of Asymmetric Polyimide Membrane for Water/Ethanol Separation in Pervaporation by the Phase Inversion Process", J. Membr. Sci., **86**(3), 231-240 (1994).

Yanagishita, H., D. Kitamoto and T. Nakane, "Separation of Alcohol Aqueous Solution by Preparation Using Asymmetric Polyimide Membrane", High Perform. Polym., **7**(3), 275-281 (1995).

Yeom, C. K. and R. Y. M. Huang, "Modelling of Pervaporation Separation of Ethanol-Water Mixtures through Crosslinked Poly(Vinyl Alcohol) Membrane", J. Membr. Sci., **67**(1), 39-55 (1992).

Zhu, Z., personal communication (1997).

Appendices

Appendix A **The observations for the fluorosilicone rubber resin and ultrafiltration polyethersulfone membrane (PES membrane) after immersed in various solvents.**

Solvents	Polyethersulfone membrane*	Fluorosilicone Rubber Resin
Methanol	No visible change was observed.	No visible change was observed.
THF	Holes were formed on the membrane, and the membrane became very brittle.	It was dissolved.
Acetic acid	No visible change was observed.	The resin viscosity was decreased but it was not dissolved.
Benzene	No visible change was observed.	The color of the resin turned milky and the viscosity did not seem to change.
Toluene	No visible change was observed.	The resin viscosity was decreased but it was not dissolved.
Chloroform	The membrane was disintegrated into globules of soft polymer precipitated at the bottom of the solvent.	The resin viscosity was decreased but it was not dissolved.
Dichrolomethane	PES was totally dissolved	The resin viscosity was decreased but it was not dissolved.
Ethyl acetate	No visible damage or swelling was detected.	It was dissolved.
Acetone	PES became translucent and swollen.	It was dissolved.
Ethanol	No visible change was observed.	No visible change was observed.

'*' Commercial ultrafiltration polyethersulfone membrane (product identification: HM18).

Appendix B **Calibration for the gas chromatography.**

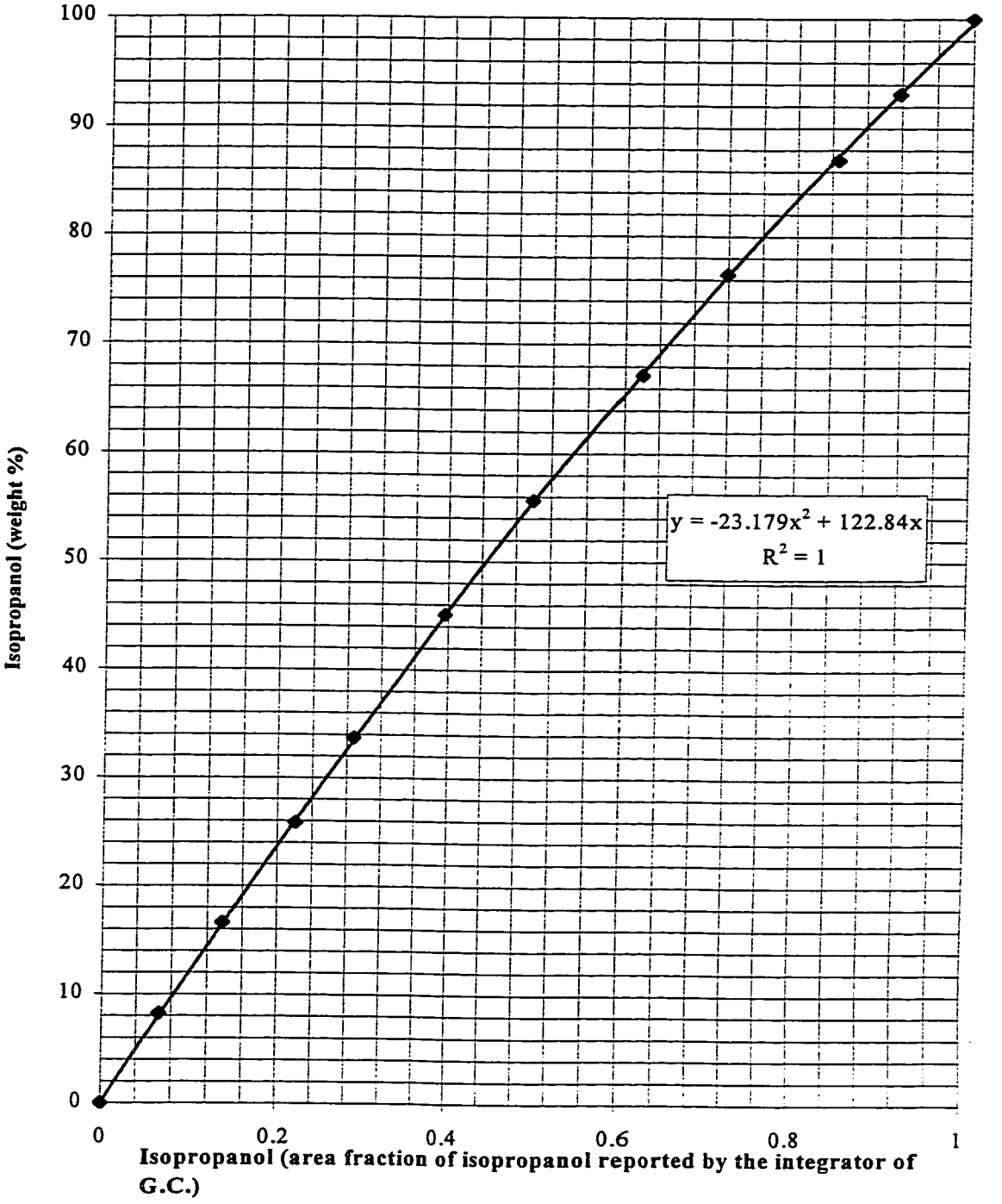

Appendix C **Infrared spectra for the Untreated PES, Undissolved PES, and chloroform.**

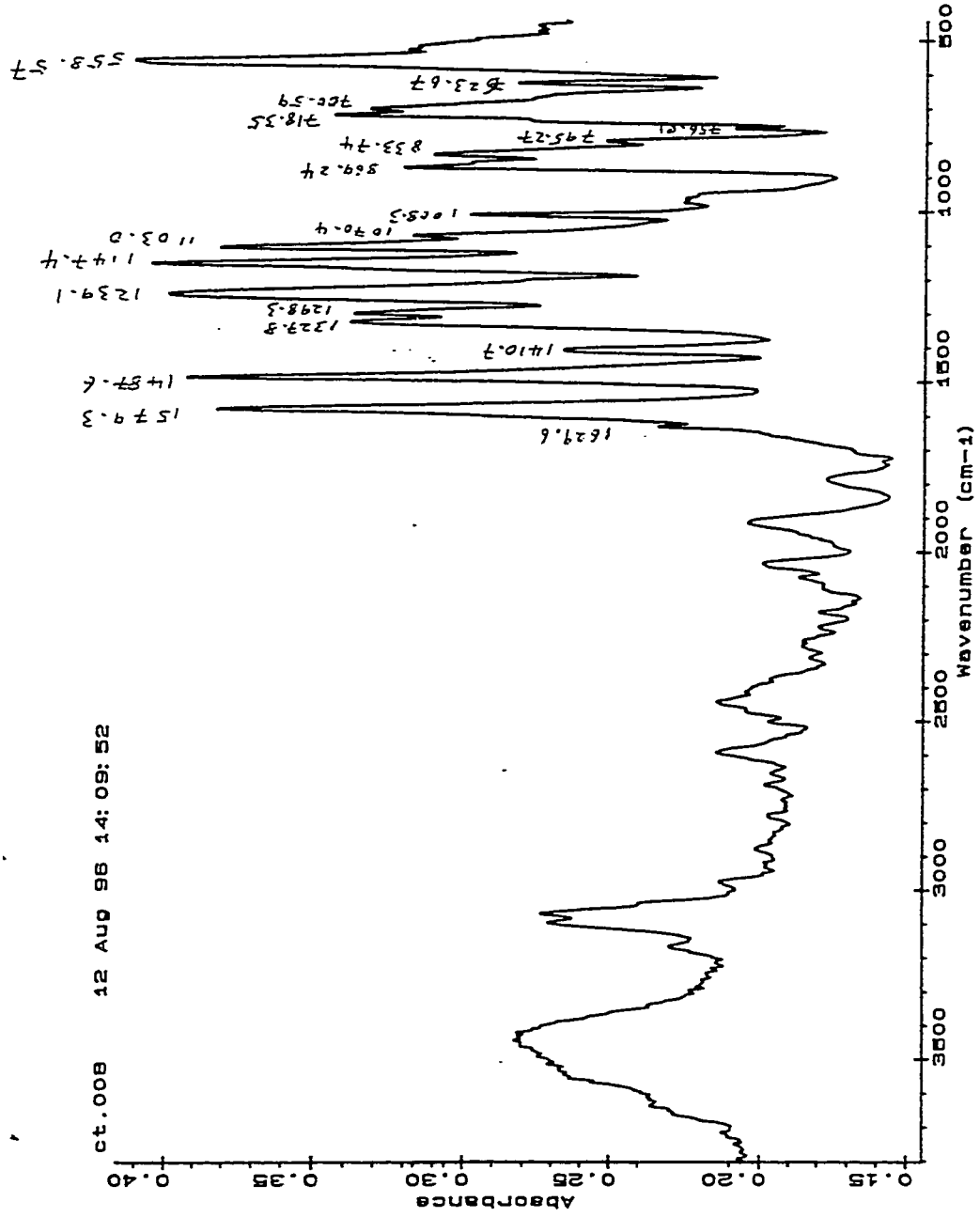

Figure AC.1 Infrared spectrum for the Untreated PES.

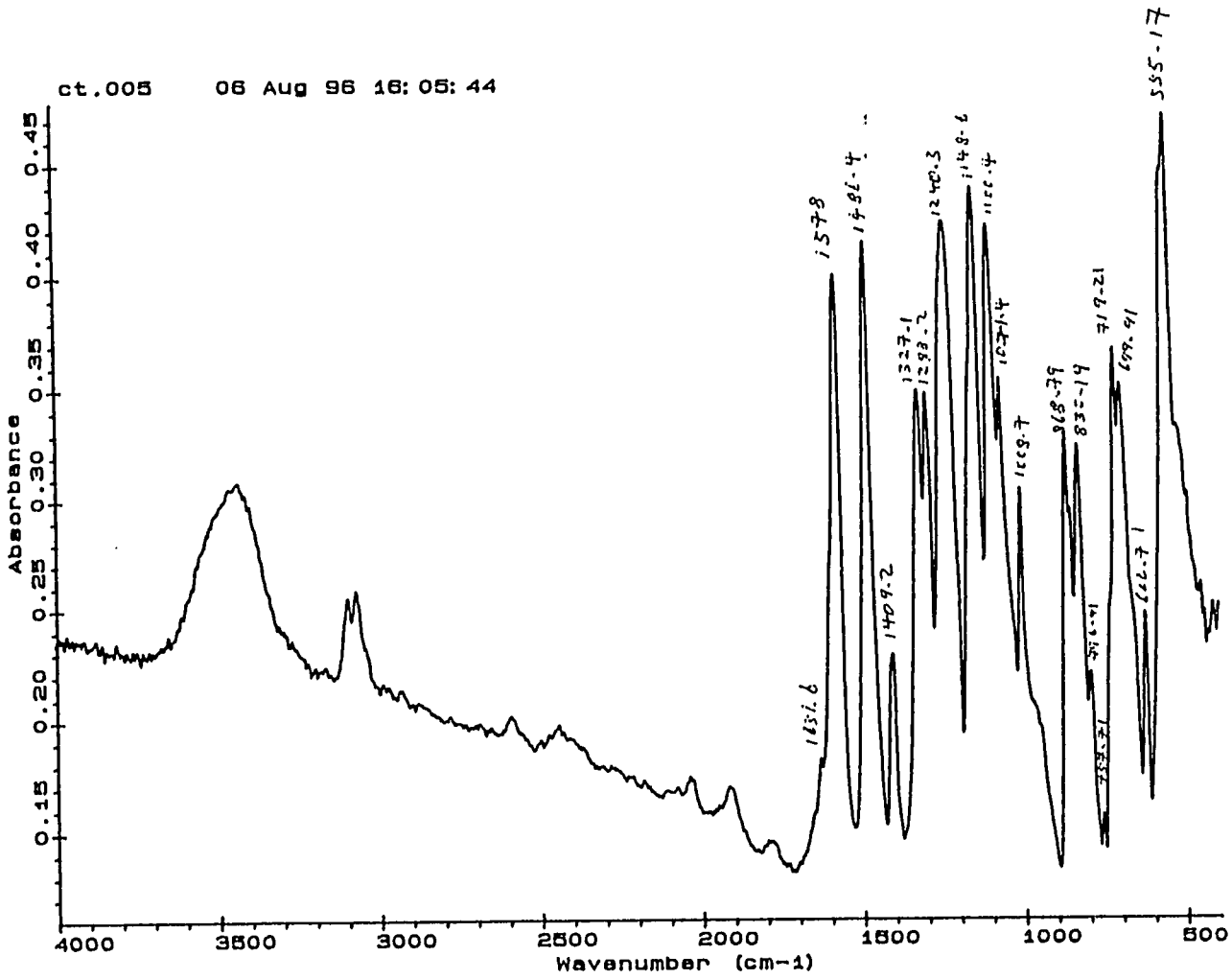

Figure AC.2 Infrared spectrum for the Undissolved PES.

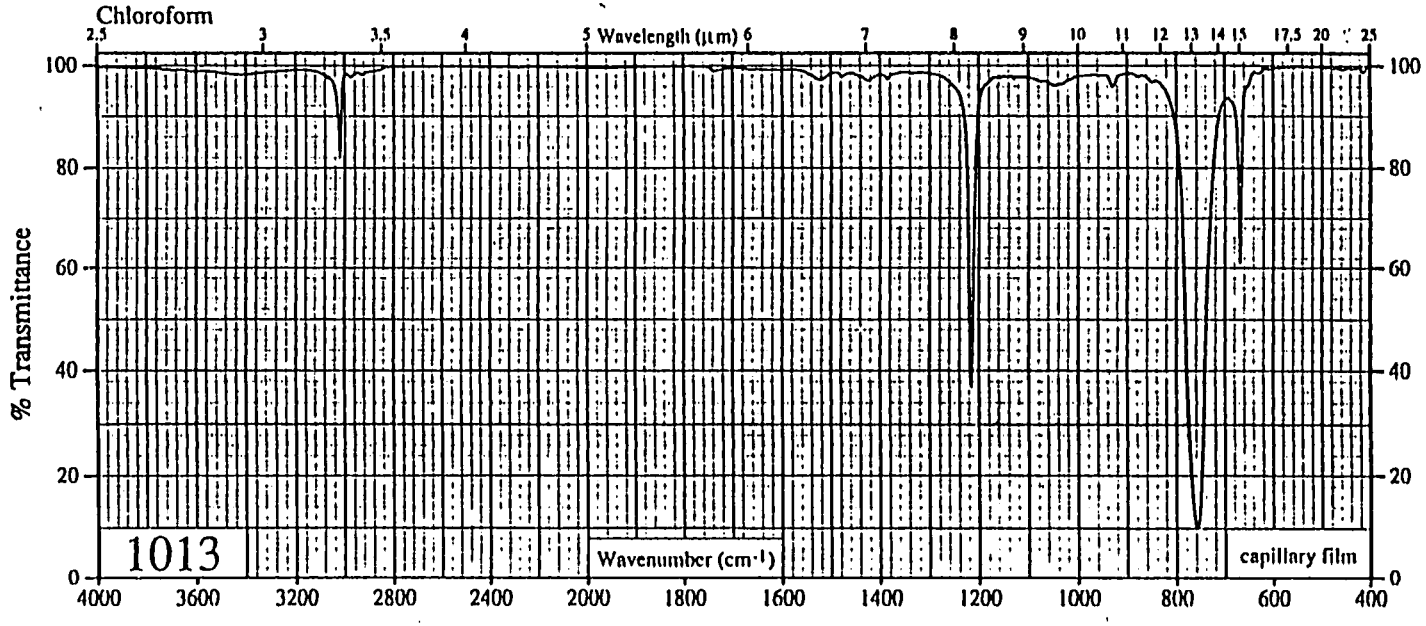

Figure AC.3 Infrared spectrum for chloroform (Brezinski, 1991).

Appendix D **Pure water permeation flux, average pure water permeation flux, and the standard deviation for PES and FPES membranes.**

Time (h)	Flux (mole/s m^2)												
	PES 1	PES 2	PES 3	PES 4	FPES 1	FPES 2	FPES 3	FPES 4	FPES 5	PES (average)	PES (std. dev.)	FPES (average)	FPES (std. dev.)
0.5	26.69	26.06	35.01	34.74	25.60	23.47	23.52	25.90	25.55	30.62	4.915	24.81	1.204
1	24.88	24.20	32.50	32.23	24.94	22.49	22.79	24.76	24.45	28.46	4.529	23.89	1.157
1.5	23.67	23.17	30.73	30.65	23.72	21.71	22.45	23.89	23.79	27.05	4.203	23.11	0.980
2	22.66	22.13	29.18	29.19	22.78	20.90	21.53	23.09	22.78	25.79	3.926	22.22	0.952
2.5	21.55	21.10	27.82	27.90	22.23	20.44	21.04	22.41	22.29	24.59	3.780	21.69	0.888
3	21.10	20.63	27.00	26.85	21.87	20.10	20.73	22.09	21.89	23.89	3.506	21.34	0.873
4	19.79	19.44	25.27	25.50	20.77	19.15	19.85	21.04	20.87	22.50	3.340	20.34	0.808
5	18.95	18.65	24.09	24.23	20.05	18.49	19.17	20.28	20.12	21.48	3.099	19.62	0.764
17	18.94	18.49	23.85	24.26	19.69	18.38	19.18	19.86	19.79	21.38	3.096	19.38	0.617
18	18.11	17.57	23.03	23.38	18.88	17.44	18.28	19.16	18.83	20.52	3.108	18.52	0.679
20	16.99	16.53	21.06	21.47	17.86	16.44	17.30	17.84	17.67	19.01	2.609	17.42	0.593
45	16.60	16.34	20.29	21.25	17.80	16.41	17.21	17.62	17.51	18.62	2.517	17.31	0.547
70	16.61	16.29	19.87	20.74	17.56	16.03	17.10	17.34	17.26	18.38	2.255	17.06	0.599
71	16.28	15.85	19.50	20.10	17.15	15.95	16.60	17.17	16.81	17.93	2.180	16.74	0.499
72	16.33	15.97	19.33	19.99	16.97	15.60	16.53	16.64	16.61	17.91	2.048	16.47	0.514
99.5	16.48	15.89	19.98	20.08	17.34	16.06	16.59	16.83	16.90	18.11	2.234	16.74	0.471
100.5	16.07	15.55	19.32	19.01	16.91	15.48	16.04	16.21	16.06	17.49	1.952	16.14	0.511
118	15.50	14.96	18.32	18.80	16.27	15.23	15.99	16.19	16.03	16.89	1.945	15.94	0.414
119	14.80	14.32	17.31	17.79	15.52	14.56	15.21	15.41	15.27	16.06	1.748	15.19	0.374
120	14.45	14.15	16.87	17.43	15.53	14.50	15.19	15.07	15.04	15.73	1.668	15.07	0.370
121	14.37	13.92	16.39	17.02	15.33	14.10	14.69	14.60	14.67	15.42	1.511	14.68	0.435
122	14.16	13.68	16.02	16.60	14.98	13.87	14.86	14.36	14.54	15.12	1.416	14.52	0.439
141.5	14.21	13.70	16.55	17.00	14.73	13.91	14.59	14.69	14.67	15.37	1.654	14.52	0.345
142.5	13.75	13.26	15.89	16.72	14.42	13.68	14.48	14.40	14.30	14.90	1.660	14.26	0.329

144.5	13.21	12.96	15.27	16.10	14.43	13.73	14.23	14.08	14.16	14.38	1.542	14.13	0.259
146.5	13.77	13.11	15.41	16.17	14.24	13.36	14.02	13.99	14.22	14.61	1.418	13.97	0.358
165.25	13.50	13.26	15.60	16.25	14.36	13.52	14.19	14.06	13.92	14.65	1.493	14.01	0.318
167.25	12.92	12.42	15.17	15.80	13.91	13.12	13.60	13.63	13.55	14.08	1.659	13.56	0.287
169.5	12.86	12.43	14.66	15.37	13.73	12.83	13.34	13.28	13.11	13.83	1.412	13.26	0.331
171	12.50	12.19	14.08	15.09	13.36	12.76	13.30	13.14	13.13	13.46	1.362	13.14	0.232
173.5	12.12	11.97	13.73	14.72	12.93	12.19	12.72	12.67	12.67	13.13	1.321	12.64	0.274
175.5	11.90	11.72	13.50	14.80	12.79	12.06	12.65	12.66	12.62	12.98	1.455	12.56	0.285
189.25	12.71	12.36	14.54	15.01	13.32	12.59	12.97	13.01	12.93	13.66	1.315	12.96	0.261
190.25	12.07	11.83	13.88	14.62	12.95	12.26	12.79	12.92	12.85	13.10	1.365	12.75	0.283
191.25	12.12	11.83	13.57	14.41	12.68	12.03	12.71	12.56	12.68	12.98	1.217	12.54	0.286
217.25	12.23	12.05	13.87	14.49	13.06	12.25	12.65	12.70	12.77	13.16	1.208	12.69	0.290
219.5	11.78	11.67	13.17	14.07	12.73	11.94	12.41	12.23	12.33	12.67	1.156	12.33	0.286
221.5	11.56	11.24	12.89	13.73	12.43	11.68	12.26	12.12	12.17	12.36	1.160	12.13	0.279
223.5	11.39	11.33	12.83	13.68	12.22	11.63	12.14	12.09	12.10	12.31	1.150	12.04	0.233
285.5	11.20	11.09	12.70	13.40	12.30	11.62	12.20	11.94	12.04	12.10	1.136	12.02	0.262
287.5	10.68	10.46	11.98	12.63	11.62	10.97	11.48	11.39	11.47	11.44	1.040	11.39	0.247
288.5	10.74	10.74	12.21	12.73	11.89	11.28	11.68	11.51	11.74	11.60	1.024	11.62	0.232
338.5	10.91	10.62	12.18	12.83	11.81	11.08	11.52	11.42	11.57	11.63	1.045	11.48	0.267
340.5	10.37	10.42	11.74	12.33	11.58	10.96	11.31	11.21	11.35	11.21	0.975	11.28	0.225
342.5	10.26	10.22	11.64	12.39	11.34	10.75	11.11	11.16	11.47	11.13	1.071	11.17	0.273
391.25	10.67	10.49	12.23	12.88	11.85	11.17	11.44	11.50	11.60	11.57	1.175	11.51	0.247
393.25	10.48	10.34	11.87	12.48	11.68	11.02	11.23	11.54	11.57	11.29	1.050	11.41	0.274
395.25	10.22	10.23	11.64	12.21	11.39	10.82	11.02	11.26	11.27	11.08	1.007	11.15	0.229
413.5	10.60	10.32	12.10	12.76	11.69	11.08	11.36	11.44	11.49	11.45	1.177	11.41	0.220
415.5	10.16	10.07	11.68	12.42	11.38	10.73	10.99	11.21	11.30	11.08	1.161	11.12	0.263
417.5	9.95	9.89	11.41	12.00	11.21	10.55	10.82	11.04	11.09	10.81	1.060	10.94	0.262
419.5	9.87	9.84	11.29	11.96	11.10	10.56	10.85	10.95	11.02	10.74	1.056	10.90	0.208
457.25	10.48	10.43	12.03	12.55	11.75	11.00	11.39	11.46	11.42	11.37	1.079	11.40	0.265
459.25	10.10	9.95	11.45	12.05	11.36	10.68	10.88	11.01	11.01	10.89	1.030	10.99	0.247
460.25	9.95	9.87	11.35	11.97	11.20	10.65	10.89	11.02	11.12	10.79	1.038	10.98	0.213
505	9.91	9.82	11.40	11.97	11.17	10.59	10.84	10.99	10.97	10.78	1.077	10.91	0.213
508	9.71	9.64	11.10	11.65	10.98	10.45	10.59	10.77	10.81	10.53	1.008	10.72	0.206

511	9.46	9.43	10.83	11.46	10.89	10.18	10.32	10.58	10.51	10.29	1.014	10.50	0.272
514	9.29	9.33	10.74	11.28	10.73	10.15	10.23	10.54	10.45	10.16	1.007	10.42	0.233
558.5	9.64	9.53	11.03	11.59	10.75	10.30	10.44	10.60	10.69	10.44	1.024	10.56	0.184
562	9.12	9.12	10.59	11.03	10.56	9.98	10.09	10.28	10.32	9.96	0.992	10.25	0.222
565	9.10	8.62	10.45	10.97	10.35	9.89	9.99	10.29	10.31	9.79	1.108	10.17	0.208
576.5	8.59	8.59	9.95	10.48	9.88	9.41	9.45	9.80	9.70	9.40	0.961	9.65	0.209
581.5	8.46	8.53	9.83	10.33	9.86	9.30	9.38	9.49	9.64	9.29	0.939	9.53	0.220
584.5	9.31	9.32	10.71	11.19	10.65	9.99	10.16	10.50	10.45	10.13	0.967	10.35	0.266
586.5	9.04	9.09	10.41	10.88	10.44	9.80	9.89	10.21	10.24	9.85	0.932	10.12	0.263
605.5	8.69	8.72	10.14	10.55	9.96	9.48	9.44	9.92	9.86	9.53	0.960	9.73	0.252
607.5	8.68	8.74	10.13	10.49	10.01	9.51	9.48	9.91	9.87	9.51	0.936	9.76	0.244
609	8.66	8.79	10.08	10.51	9.98	9.47	9.48	9.87	9.87	9.51	0.924	9.73	0.241
623	8.48	8.56	9.84	10.26	9.63	9.20	9.27	9.82	9.52	9.28	0.903	9.49	0.257
626	8.63	8.66	9.92	10.39	9.75	9.34	9.33	9.64	9.67	9.40	0.893	9.55	0.199
648.5	7.95	8.03	9.18	9.63	8.95	8.53	8.67	8.92	8.87	8.70	0.840	8.79	0.181
652	7.82	7.91	9.00	9.45	8.82	8.45	8.55	8.76	8.71	8.54	0.807	8.66	0.154
670.25	7.73	7.81	8.87	9.34	8.64	8.29	8.39	8.63	8.54	8.44	0.796	8.50	0.153
671.25	7.76	7.85	8.90	9.34	8.68	8.32	8.49	8.60	8.58	8.46	0.783	8.54	0.136
672	6.06	6.09	6.92	7.23	6.71	6.37	6.47	6.62	6.64	6.57	0.589	6.56	0.136
672.25	6.17	6.22	7.00	7.32	6.75	6.45	6.55	6.69	6.71	6.68	0.573	6.63	0.127
672.5	6.19	6.34	7.04	7.36	6.83	6.49	6.59	6.75	6.74	6.73	0.558	6.68	0.137
672.75	6.24	6.36	7.10	7.45	6.90	6.55	6.61	6.79	6.84	6.79	0.582	6.74	0.152
673	6.24	6.32	7.07	7.41	6.84	6.49	6.57	6.71	6.76	6.76	0.574	6.67	0.140
673.5	6.26	6.35	7.11	7.45	6.88	6.55	6.63	6.80	6.83	6.79	0.584	6.74	0.142
674	6.23	6.34	7.08	7.44	6.85	6.50	6.59	6.76	6.80	6.77	0.582	6.70	0.148
675	6.26	6.33	7.13	7.47	6.86	6.55	6.62	6.80	6.83	6.80	0.597	6.73	0.139
677	6.22	6.34	7.09	7.45	6.86	6.55	6.62	6.81	6.81	6.78	0.593	6.73	0.137
680	6.24	6.33	7.14	7.46	6.89	6.55	6.62	6.81	6.83	6.79	0.600	6.74	0.148
695	6.28	6.34	7.17	7.49	6.88	6.57	6.64	6.84	6.80	6.82	0.603	6.75	0.134
722	6.49	6.53	7.41	7.70	7.11	6.76	6.81	7.06	7.00	7.03	0.613	6.95	0.153
815	6.64	6.68	7.55	7.83	7.24	6.87	6.94	7.19	7.12	7.18	0.609	7.07	0.161

Flow-rate of the feed = 2.2 L/min, temperature = ambient (25°C, and operating temperature = 70 psi (482631 Pa), switch to 50 psi (344737 Pa) after 672 hours

Appendix E **Product rate of PEG solution for PES and FPES membranes obtained from ultrafiltration experiment.**

Molecular weight of PEG	Product rate (mole/s m^2)								
	PES 1	PES 2	PES 3	PES 4	FPES 1	FPES 2	FPES 3	FPES 4	FPES 5
1500	7.16	7.25	8.12	8.34	7.64	7.29	7.42	7.63	7.61
3000	7.01	7.12	7.85	8.10	7.28	6.98	7.16	7.36	7.29
6000	5.99	6.07	6.35	6.66	5.78	5.59	5.98	6.06	5.94
12000	4.2	4.41	4.39	4.67	4.00	3.98	4.16	4.11	4.01
20000	4.01	4.21	4.19	4.47	3.82	3.81	4.00	3.91	3.84
35000	3.43	3.63	3.57	3.90	3.25	3.27	3.39	3.42	3.26

Flow-rate of the feed = 2.2 L/min, temperature = ambient (25°C), and operating pressure = 50 psig (345 kPa)

Appendix F **Solute rejection for the polyethylene glycol solutions.**

Molecular weight of PEG	Solute rejection (%)								
	PES 1	PES 2	PES 3	PES 4	FPES 1	FPES 2	FPES 3	FPES 4	FPES 5
1500	1%	3%	2%	1%	0%	1%	1%	0%	0%
3000	8%	9%	6%	5%	6%	8%	6%	5%	4%
6000	40%	43%	38%	35%	43%	45%	40%	38%	38%
12000	78%	80%	78%	71%	78%	78%	78%	75%	77%
20000	83%	85%	83%	75%	83%	83%	83%	81%	82%
35000	87%	88%	87%	77%	86%	85%	86%	82%	85%

Flow-rate of the feed = 2.2 L/min, temperature = ambient (25°C), and operating pressure = 50 psig (345 kPa)

Appendix G Average product rates, average percentage solute rejections, and standard deviations for each PEG solution.

Molecular weight of PEG in solution	PES membrane		FPES membrane	
	Average product rate (mole/s m^2)	Average solute rejection (%)	Average product rate (mole/s m^2)	Average solute rejection (%)
1500	7.72 (S.D. = 0.60)	2 (S.D. = 1)	7.52 (S.D. = 0.15)	0 (S.D. = 1)
3000	7.52 (S.D. = 0.54)	7 (S.D. = 2)	7.21 (S.D. = 0.15)	6 (S.D. = 2)
6000	6.27 (S.D. = 0.31)	39 (S.D. = 4)	5.87 (S.D. = 0.19)	41 (S.D. = 3)
12000	4.42 (S.D. = 0.19)	77 (S.D. = 4)	4.05 (S.D. = 0.08)	77 (S.D. = 2)
20000	4.22 (S.D. = 0.19)	82 (S.D. = 5)	3.88 (S.D. = 0.08)	82 (S.D. = 1)
35000	3.63 (S.D. = 0.19)	85 (S.D. = 5)	3.32 (S.D. = 0.08)	85 (S.D. = 2)

S.D. = standard deviation

Flow-rate of the feed = 2.2 L/min, temperature = ambient (25°C), and operating pressure = 50 psig (345 kPa)

Appendix H **Pure water permeation flux for PES and FPES membranes during the polyethylene glycol solution experiment.**

Time (h)	Pure water permeation flux (mole/s m^2)												
	PES 1	PES 2	PES 3	PES 4	FPES 1	FPES 2	FPES 3	FPES 4	FPES 5	PES (average)	PES (std. dev.)	FPES (average)	FPES (std. dev.)
815	6.638	6.676	7.553	7.833	7.239	6.866	6.943	7.192	7.124	7.175	0.609	7.073	0.161
892.000	6.744	6.813	7.671	7.936	7.286	6.987	7.027	7.301	7.208	7.291	0.602	7.162	0.146
1041.750	6.918	7.038	7.881	8.098	7.466	7.145	7.189	7.472	7.368	7.484	0.593	7.328	0.153
1079.000	7.158	7.233	8.119	8.328	7.677	7.36	7.376	7.671	7.587	7.709	0.600	7.534	0.156
1083.000	7.393	7.438	8.359	8.568	7.853	7.512	7.586	7.815	7.747	7.939	0.611	7.703	0.148
1085.750	7.437	7.503	8.422	8.630	7.533	7.490	7.605	7.862	7.777	7.998	0.616	7.654	0.160
1088.580	7.502	7.567	8.521	8.700	7.904	7.506	7.597	7.941	7.843	8.072	0.626	7.758	0.195
1102.250	7.414	7.506	8.464	8.601	7.828	7.430	7.468	7.844	7.732	7.996	0.623	7.660	0.198
1107.750	7.165	7.245	8.121	8.236	7.438	7.055	7.033	7.532	7.364	7.692	0.565	7.284	0.227
1110.750	7.280	7.357	8.305	8.463	7.644	7.239	7.132	7.806	7.56	7.851	0.619	7.476	0.282
1114.750	7.322	7.194	8.129	8.294	7.451	7.036	6.851	7.566	7.355	7.735	0.557	7.252	0.298

Flow-rate of the feed = 2.2 L/min, temperature = ambient (25°C), and operating pressure = 50 psig (345 kPa)

Appendix I Pure Permeate flux versus downstream pressure for homogeneous fluorosilicone rubber membrane.

Distilled water flux (mole/m^2 s)			Isopropyl alcohol flux (mole/m^2 s)		
Downstream Pressure (Pa)	Experimental	Pore model	Downstream pressure (Pa)	Experimental	Pore model
159.99	0.000179	0.000158	159.99	0.000152	0.000149
906.59	0.000136	0.000144	1439.88	0.000142	0.000140
1626.53	0.000094	0.000112	2706.44	0.000107	0.000115
2359.81	0.000049	0.000061	3973.01	0.000807	0.000076
2737	-	0.000027	4986	-	0.000033
3093.08	0.000042	0.0000269	5252.9	0.000045	0.0000329
3666.37	0.000030	0.0000268	5679.53	0.000046	0.0000327
5332.89	0.000020	0.0000263	6666.11	0.000026	0.0000324
7999.34	0.000012	0.0000256	7999.34	0.000013	0.000032

Temperature = 23°C

Appendix J **Experimental and pore model results for the pervaporation test of composite fluorosilicone rubber membrane with distilled water and isopropyl alcohol feed mixture.**

Experimental result			Vapor-liquid equilibrium predicted by Margules Correlation		Permeate composition and flux predicted by the Pore Model		
Water			Water		Water		
Feed	Permeate	Mixture flux	Liquid phase	Vapor phase	Feed	Permeate	Mixture flux
mole%	mole%	mole/m^2 s	mole%	mole%	mole%	mole%	mole/m^2 s
0	0	0.000152	0	0	0	0.000	0.000102
0.134	0.312	0.000176	0.05	0.069	0.05	0.025	0.000094
0.52	0.630	0.000204	0.1	0.138	0.1	0.106	0.000092
0.767	0.724	0.000211	0.15	0.202	0.15	0.231	0.000095
0.908	0.800	0.000169	0.2	0.260	0.2	0.366	0.000103
0.984	0.957	0.000167	0.25	0.310	0.25	0.484	0.000114
1	1	0.000179	0.3	0.351	0.3	0.577	0.000125
			0.35	0.384	0.35	0.645	0.000136
			0.4	0.409	0.4	0.691	0.000145
			0.45	0.428	0.45	0.723	0.000151
			0.5	0.44	0.5	0.742	0.000155
			0.55	0.447	0.55	0.753	0.000157
			0.6	0.450	0.6	0.757	0.000158
			0.65	0.449	0.65	0.756	0.000158
			0.7	0.447	0.7	0.753	0.000157
			0.75	0.445	0.75	0.75	0.000157
			0.8	0.447	0.8	0.753	0.000157
			0.85	0.459	0.85	0.77	0.000156
			0.9	0.494	0.9	0.816	0.000152
			0.95	0.594	0.95	0.908	0.000145
			1	1	1	1	0.000143

Downstream pressure = 160 Pa (1.2 torrs), and temperature = 23°C

IMAGE EVALUATION TEST TARGET (QA-3)

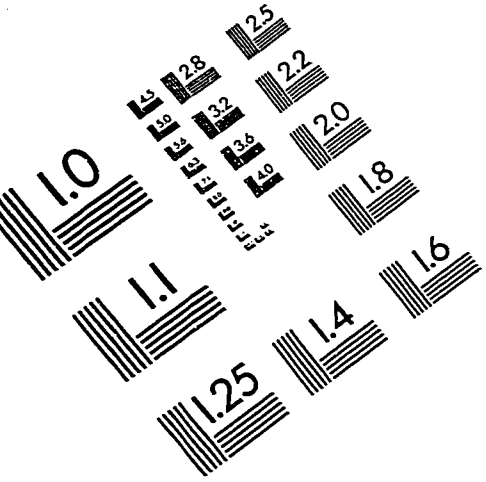

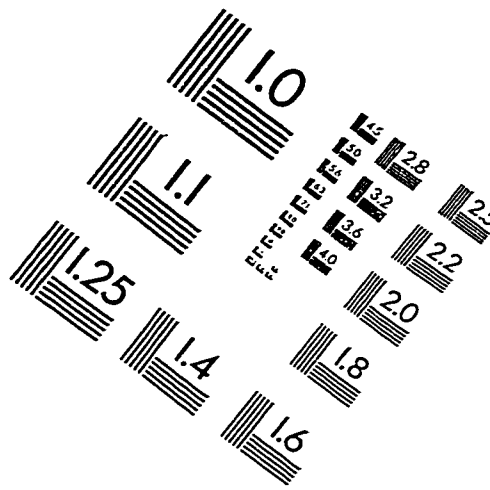

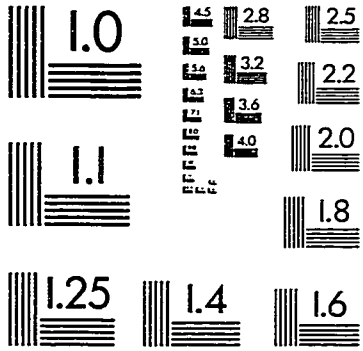

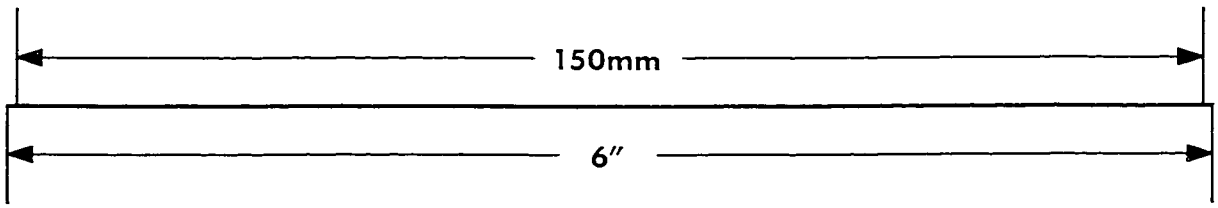

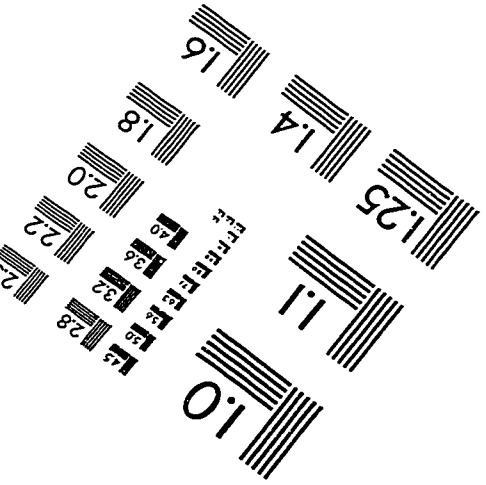

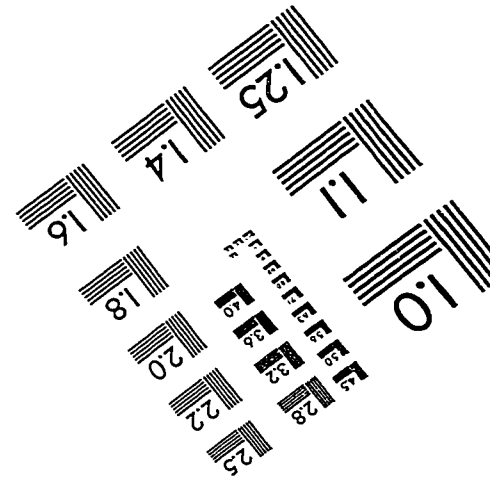

APPLIED IMAGE, Inc
1653 East Main Street
Rochester, NY 14609 USA
Phone: 716/482-0300
Fax: 716/288-5989